ELSEVIER

Contents lists available at ScienceDirect

Applied Energy

journal homepage: www.elsevier.com/locate/apenergy



Potassium carbonate impregnation and torrefaction of wood block for thermal properties improvement: Prediction of torrefaction performance using artificial neural network

Larissa Richa ^a, Baptiste Colin ^a, Anélie Pétrissans ^{a,*}, Ciera Wallace ^b, Jasmine Wolfgram ^b, Rafael L. Quirino ^b, Wei-Hsin Chen ^{c,d,e,**}, Mathieu Pétrissans ^a

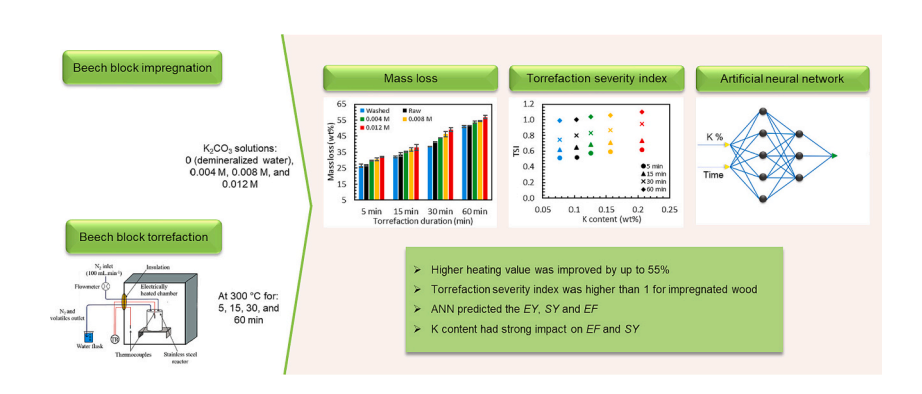
- ^a Université de Lorraine, INRAE, LERMaB, F-88000 Epinal, France
- ^b Chemistry Department, Georgia Southern University, Statesboro GA-30460, USA
- ^c Department of Aeronautics and Astronautics, National Cheng Kung University, Tainan 701, Taiwan
- ^d Research Center for Smart Sustainable Circular Economy, Tunghai University, Taichung 407, Taiwan
- ^e Department of Mechanical Engineering, National Chin-Yi University of Technology, Taichung 411, Taiwan

HIGHLIGHTS

Catalytic torrefaction of wood block reduces up to 67% of torrefaction duration.

- The scale-up of the wood block with Kimpregnation and torrefaction was successful.
- Potassium improved the torrefaction severity index by up to 10%.
- Wood's thermal properties after torrefaction and K-impregnation were comparable to coal.
- Artificial neural network predicted the SY, EY, and EF with $R^2 > 0.99$.

GRAPHICAL ABSTRACT



ARTICLE INFO

Keywords:
Wood block
Potassium carbonate catalyst
Torrefaction and biochar
Artificial neural network (ANN)
Torrefaction severity index (TSI)

ABSTRACT

Catalytic torrefaction using potassium carbonate (K_2CO_3) impregnation is a pretreatment method demonstrated to catalyze wood powder's thermal degradation for energy use. In this study, beech wood boards were impregnated with K_2CO_3 , with the aim to scale up from the studies on wood powder found in the literature. The beech boards were impregnated with five different concentrations and torrefied at 300°C for four durations (5–60 min). The impregnation procedure was successful with a linear increase of K content in wood from 0.103 wt% for raw to 0.207 wt% for the 0.012 M sample. The weight loss during torrefaction increased with the increasing potassium (K) content in wood, reaching a maximum increase of 27.17% between 0.012 M and washed (no K_2CO_3) after 30 min. For the longest duration, the extent of the catalytic action of K decreased, similar to what is observed in wood powder. After 60 min torrefaction, potassium increased the torrefaction severity index by up to 10% and the higher heating value (*HHV*) by up to 55%. Potassium efficiently increased

^{*} Corresponding author.

^{**} Corresponding author at: Department of Aeronautics and Astronautics, National Cheng Kung University, Tainan 701, Taiwan. E-mail addresses: anelie.petrissans@univ-lorraine.fr (A. Pétrissans), weihsinchen@gmail.com, chenwh@mail.ncku.edu.tw (W.-H. Chen).

the fixed carbon and decreased the volatile matter to values comparable to coal by catalyzing the devolatilization during torrefaction. The atomic H/C and O/C ratios shifted to similar ratios as coal. The energy yield (EY) was above 80% for the shorter durations but dropped drastically at 30 and 60 min torrefaction. The prediction of the solid yield (EY), energy yield (EY), and enhancement factor of the EY0 through an artificial neural network was robust with a fit quality EY0.999. The proposed method for catalytic torrefaction on wood boards was efficient and could be used prior to grinding and transportation for bioenergy production. This process could decrease the production costs of biomass fuel to compete with fossil fuels.

O Oxygen impregnated sample to the EY of the raw one (%) H Hydrogen REF Relative enhancement factor is the ratio between the EF	Nomenc	lature	Mn	Manganese
GHG Greenhouse gas HHV Higher heating value (MJ.kg ⁻¹) Torrefaction severity index EY Energy yield (%) EFF Enhancement factor of HHV ANN Artificial neural network ICP-AES Inductively coupled plasma atomic emission spectroscopy db Dry basis AC Ash content (wt% db) FC Fixed carbon content (wt% db) TR Temperature recorder Molecules CHG (MJ.kg ⁻¹) K/K + Potassium / Potassium ion K/Cl Potassium carbonate KCl Potassium carbonate CO ₂ Carbon dioxide Symbols IP Impregnation percentage of the solution in the wood blow (%) IRK Impregnation ratio of potassium in the wood compared the raw (db) WL Weight loss (wt% db) FC Fixed carbon content (wt% db) TR Temperature recorder Molecules C Carbon O Oxygen H Hydrogen REF Relative energy yield is the ratio between the EY of the impregnated sample to the EY of the raw one (%) REF Relative enhancement factor is the ratio between the EF			Mg	Magnesium
HHVHigher heating value (MJ.kg $^{-1}$)K / K $^{+}$ Potassium / Potassium ionTSITorrefaction severity indexKClPotassium carbonateEYEnergy yield (%)K2CO3Potassium carbonateEFEnhancement factor of HHVCO2Carbon dioxideSYSolid yield (wt%)SymbolsANNArtificial neural networkIPImpregnation percentage of the solution in the wood bloody (%)ICP-AESInductively coupled plasma atomic emission spectroscopy dbIPImpregnation percentage of the solution in the wood bloody (%)ACAsh content (wt% db)IRKImpregnation ratio of potassium in the wood compared the raw (db)VMVolatile matter content (wt% db)WIWeight loss (wt% db)FCFixed carbon content (wt% db) σ Pearson standard deviationTemperature recorderRSYRelative solid yield is the ratio between the SY of the impregnated sample to the SY of the raw one (%)MoleculesREYRelative energy yield is the ratio between the EY of the impregnated sample to the EY of the raw one (%)CCarbonREFRelative enhancement factor is the ratio between the EF	Abbreviation		Ca	Calcium
TSITorrefaction severity indexKClPotassium chlorideEYEnergy yield (%)K2CO3Potassium carbonateEFEnhancement factor of HHVCO2Carbon dioxideSYSolid yield (wt%)SymbolsANNArtificial neural networkIPImpregnation percentage of the solution in the wood bloomy (%)ICP-AESInductively coupled plasma atomic emission spectroscopy dbIRImpregnation ratio of potassium in the wood compared the raw (db)ACAsh content (wt% db)IRImpregnation ratio of potassium in the wood compared the raw (db)VMVolatile matter content (wt% db)WLWeight loss (wt% db)FCFixed carbon content (wt% db)σPearson standard deviationTemperature recorderRSYRelative solid yield is the ratio between the SY of the impregnated sample to the SY of the raw one (%)MoleculesCCarbonREYRelative energy yield is the ratio between the EY of the impregnated sample to the EY of the raw one (%)CCarbonREFRelative enhancement factor is the ratio between the EF	GHG	Greenhouse gas	Na	Sodium
EY Energy yield (%) EF Enhancement factor of HHV CO2 Carbon dioxide SY Solid yield (wt%) ANN Artificial neural network ICP-AES Inductively coupled plasma atomic emission spectroscopy db Dry basis AC Ash content (wt% db) FC Fixed carbon content (wt% db) TR Temperature recorder Molecules C Carbon O Oxygen H Hydrogen K2CO3 Potassium carbonate CO2 Carbon dioxide Symbols IP Impregnation percentage of the solution in the wood blow (%) Impregnation ratio of potassium in the wood compared the raw (db) WL Weight loss (wt% db) FR Relative solid yield is the ratio between the SY of the impregnated sample to the SY of the raw one (%) REY Relative energy yield is the ratio between the EY of the impregnated sample to the EY of the raw one (%) REF Relative enhancement factor is the ratio between the EF	HHV	Higher heating value (MJ.kg ⁻¹)	K / K^+	Potassium / Potassium ion
EFEnhancement factor of HHVCO2Carbon dioxideSYSolid yield (wt%)SymbolsANNArtificial neural networkIPImpregnation percentage of the solution in the wood blow (%)ICP-AESInductively coupled plasma atomic emission spectroscopy dbIPImpregnation percentage of the solution in the wood blow (%)ACAsh content (wt% db)IR _K Impregnation ratio of potassium in the wood compared the raw (db)VMVolatile matter content (wt% db)WLWeight loss (wt% db)FCFixed carbon content (wt% db)WLWeight loss (wt% db)TRTemperature recorderσPearson standard deviationRSYRelative solid yield is the ratio between the SY of the impregnated sample to the SY of the raw one (%)CCarbonREYRelative energy yield is the ratio between the EY of the impregnated sample to the EY of the raw one (%)OOxygenimpregnated sample to the EY of the raw one (%)HHydrogenREFRelative enhancement factor is the ratio between the EF	TSI	Torrefaction severity index	KCl	Potassium chloride
SYSolid yield (wt%)SymbolsANNArtificial neural networkIPImpregnation percentage of the solution in the wood blow (%)IDP DescriptionImpregnation percentage of the solution in the wood blow (%)IDP DescriptionImpregnation ratio of potassium in the wood compared the raw (db)IDP DescriptionImpregnation ratio of potassium in the wood compared the raw (db)IDP DescriptionImpregnation ratio of potassium in the wood compared the raw (db)IDP DescriptionImpregnation ratio of potassium in the wood compared the raw (db)IDP DescriptionWL Weight loss (wt% db)IDP DescriptionImpregnation ratio of potassium in the wood compared the raw (db)IDP DescriptionWL Weight loss (wt% db)IDP DescriptionRESY Relative solid yield is the ratio between the SY of the impregnated sample to the SY of the raw one (%)IDP DescriptionRESY Relative energy yield is the ratio between the EY of the impregnated sample to the EY of the raw one (%)IDP DescriptionRESY Relative enhancement factor is the ratio between the EY of the raw one (%)IDP DescriptionRESY Relative enhancement factor is the ratio between the ESY of the raw one (%)	EY	Energy yield (%)	K_2CO_3	Potassium carbonate
ANN Artificial neural network ICP-AES Inductively coupled plasma atomic emission spectroscopy db Dry basis AC Ash content (wt% db) FC Fixed carbon content (wt% db) TR Temperature recorder Molecules C Carbon O Oxygen H Hydrogen ANN Artificial neural network IP Impregnation percentage of the solution in the wood blow (%) IP Impregnation ratio of potassium in the wood compared the raw (db) WL Weight loss (wt% db) FC Fixed carbon content (wt% db) FC Fixed ca	EF	Enhancement factor of HHV	CO_2	Carbon dioxide
ICP-AES Inductively coupled plasma atomic emission spectroscopy db Dry basis AC Ash content (wt% db) FC Fixed carbon content (wt% db) TR Temperature recorder Molecules C Carbon C Oxygen H Hydrogen MIRK Impregnation percentage of the solution in the wood blog (%) IRK Impregnation ratio of potassium in the wood compared the raw (db) WL Weight loss (wt% db) FC Pearson standard deviation RSY Relative solid yield is the ratio between the SY of the impregnated sample to the SY of the raw one (%) REY Relative energy yield is the ratio between the EY of the impregnated sample to the EY of the raw one (%) REF Relative enhancement factor is the ratio between the EF	SY	Solid yield (wt%)		
The companies of the c	ANN	Artificial neural network		
AC Ash content (wt% db) WU Volatile matter content (wt% db) FC Fixed carbon content (wt% db) TR Temperature recorder Wolecules C Carbon O Oxygen H Hydrogen FIX Ash content (wt% db) IR_K Impregnation ratio of potassium in the wood compared the raw (db) WL Weight loss (wt% db) FC Pearson standard deviation FC Relative solid yield is the ratio between the SY of the impregnated sample to the SY of the raw one (%) FC Relative energy yield is the ratio between the EY of the impregnated sample to the EY of the raw one (%) FC Relative enhancement factor is the ratio between the EF Relative enhancement factor is the ratio between the EF	ICP-AES	Inductively coupled plasma atomic emission spectroscopy	IΡ	1 0 1 0
VM Volatile matter content (wt% db) FC Fixed carbon content (wt% db) TR Temperature recorder Molecules C Carbon O Oxygen H Hydrogen WL Weight loss (wt% db) Fearson standard deviation RSY Relative solid yield is the ratio between the SY of the impregnated sample to the SY of the raw one (%) REY Relative energy yield is the ratio between the EY of the impregnated sample to the EY of the raw one (%) REF Relative enhancement factor is the ratio between the EF	db	Dry basis		
FC Fixed carbon content (wt% db) TR Temperature recorder Molecules C Carbon O Oxygen H Hydrogen WL Weight loss (wt% db) Fearson standard deviation RSY Relative solid yield is the ratio between the SY of the impregnated sample to the SY of the raw one (%) REY Relative energy yield is the ratio between the EY of the impregnated sample to the EY of the raw one (%) REF Relative enhancement factor is the ratio between the EF	AC	Ash content (wt% db)	IR_K	1 0 1
TR Temperature recorder σ Pearson standard deviation RSY Relative solid yield is the ratio between the SY of the impregnated sample to the SY of the raw one (%) C Carbon O Oxygen H Hydrogen σ Pearson standard deviation RSY Relative solid yield is the ratio between the SY of the raw one (%) REY Relative energy yield is the ratio between the EY of the impregnated sample to the EY of the raw one (%) REF Relative enhancement factor is the ratio between the EF	VM	Volatile matter content (wt% db)		
RSY Relative solid yield is the ratio between the SY of the impregnated sample to the SY of the raw one (%) C Carbon REY Relative energy yield is the ratio between the EY of the O Oxygen impregnated sample to the EY of the raw one (%) H Hydrogen REF Relative enhancement factor is the ratio between the EF	FC	Fixed carbon content (wt% db)	WL	0
RSY Relative solid yield is the ratio between the SY of the impregnated sample to the SY of the raw one (%) C Carbon REY Relative energy yield is the ratio between the EY of the one of the impregnated sample to the EY of the raw one (%) H Hydrogen REF Relative enhancement factor is the ratio between the EF	TR	Temperature recorder	σ	
C Carbon REY Relative energy yield is the ratio between the EY of the O Oxygen impregnated sample to the EY of the raw one (%) H Hydrogen REF Relative enhancement factor is the ratio between the EF		1	RSY	Relative solid yield is the ratio between the <i>SY</i> of the
O Oxygen impregnated sample to the EY of the raw one (%) H Hydrogen REF Relative enhancement factor is the ratio between the EF	Molecules	:		impregnated sample to the SY of the raw one (%)
H Hydrogen REF Relative enhancement factor is the ratio between the EF	C	Carbon	REY	Relative energy yield is the ratio between the <i>EY</i> of the
	O	Oxygen		impregnated sample to the EY of the raw one (%)
N N N 1 1 1 1 1 1 1 1 1 1 1 1 1 1 1 1 1	Н	Hydrogen	REF	Relative enhancement factor is the ratio between the EF of
N Nitrogen the impregnated sample to the EF of the raw one (%)	N	Nitrogen		the impregnated sample to the EF of the raw one (%)

1. Introduction

Establishing renewable energy sources is critical with the rising concern of the global energy crisis. The energy demand is surging, and fossil-fuel extraction costs are increasing, leading to a peak in fuel costs [1]. Therefore, renewable energy, including biomass energy, is an effective substitute for depleting conventional fuel sources [2]. Using biomass fuel such as wood is considered clean energy due to its low greenhouse gases (GHG) emissions [3]. However, biomass energy needs to be affordable to compete with conventional fuel and, therefore, requires process optimization. Thermochemical conversion methods are developed to upgrade the biomass' properties according to the desired product characteristics. These methods include but are not limited to pyrolysis [4] and hydrothermal carbonization [5,6]. Torrefaction is proposed as wood pretreatment to withstand environmental conditions and to increase the solid biofuel's quality [7]. During torrefaction, the biomass is heated in an inert atmosphere (vacuum, nitrogen, flue gas, etc.) at a temperature range of 200-300°C [8]. This method induces thermochemical reactions that increase wood's homogeneity, higher heating value (HHV), and hydrophobicity. Meanwhile, torrefaction reduces wood's density and moisture content [7,9]. It impacts the mechanical properties of biomass by facilitating the particle size reduction in a narrower range and decreasing the tensile strength while increasing friability [10]. These changes in properties improve the upgraded biofuel's grinding, storage, and transportation. By facilitating grindability, torrefaction reduces the energy consumption linked to particle size reduction [11]. Manouchehrinejad et al. [12] stated that torrefying wood prior to grinding reduces the energy required for grinding by up to 90%, reducing production costs substantially. Moreover, studies showed that torrefied wood pellets have a lower energy density than untreated

pellets. This results in lower transportation and fuel production costs compared to untreated pellets [13]. Torrefaction pretreatment produces a more thermally-stable lignocellulosic biomass [14], making it more suitable for storage. Moreover, the transportation and combustion of torrefied wood emit a significantly lower quantity of greenhouse gases (GHG) than untreated wood [15]. This means that torrefying wood prior to grinding and transportation for heat and power generation could be a viable solution to reduce biofuel prices and even replace coal [16]. Torrefied biomass is recommended in co-firing and has the potential to completely replace coal without decreasing the boiler's efficiency [17].

Potassium (K) is essential for plant growth and improves photosynthesis' CO₂ fixation [18]. Its presence in greenwood is in ionic form (K⁺) [19]. Potassium can be added to lignocellulosic biomass by impregnating small wood particles or powder [20]. Then, the drying after impregnation can be achieved at a low cost using low-temperature waste heat, accounting for 60% of the dissipated heat in energy production processes [21]. Potassium is an alkali catalyst that influences the dynamics and products of pyrolyzed biomass [22]. Hwang et al. [23] noticed a char yield increase with the increase of potassium content during pyrolysis. According to Guo et al. [24], the K-impregnation of pine wood largely increases the gas yield and reduces tar formation during pyrolysis. During the combustion of wood particles, potassium impacts the ignition delay and volatile combustion times [25]. However, minerals' devolatilization at high temperatures increases corrosion risks and slagging behavior. Therefore, the operating temperatures should not exceed 750-850 °C, depending on the desired application, to avoid K devolatilization [26]. This temperature range is considered sage for Kcatalyzed thermal processes to produce high-quality biochar, activated carbon, or fertilizer [27–29]. At torrefaction temperatures, potassium addition affects the thermal degradation kinetics of wood powder by accelerating weight loss [30]. Silveira et al. [31] found that increasing

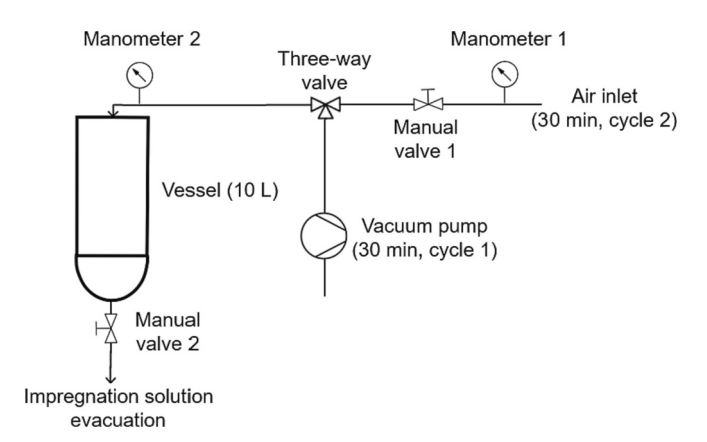


Fig. 1. Wood blocks impregnation process diagram.

potassium content in wood decreased the maximum degradation temperature, mainly attributed to cellulose. The catalytic effect of potassium in wood's torrefaction is attributed to its actions of cleaving hydrogen bonds in cellulose and cleaving C—C bonds and glycosidic linkages [32].

The torrefaction severity index (*TSI*) is a crucial indicator to measure the impact of torrefaction on biomass thermodegradation [33]. When the torrefaction extent increases, the thermal properties of wood change. This change is evaluated by the determination of the energy yield (*EY*) and higher heating value (*HHV*) [34,35]. The energy yield depends on the enhancement factor of the *HHV* (*EF*) and the solid yield (*SY*) of the torrefied biomass relative to the raw [36]. The beforementioned parameters are essential to evaluate a biofuel's energy performance and correlate it to different torrefaction conditions such as temperature, duration, catalyst, etc. Therefore, with the desire to predict torrefaction performance, machine learning has recently become a popular approach. Different methods exist, including artificial neural networks (ANNs), multivariate adaptive regression splines (MARS), and decision tree [35,36]. The most commonly used method for biomass torrefaction is ANN which results in accurate predictions in most cases [38,39].

To the authors' knowledge, all studies of potassium's effect on wood torrefaction were limited to the impregnation of wood powder [40–42]. However, the upscaling of the process needs to be studied because biomass behavior is different between laboratory and industrial scales. For example, different wood particle sizes lead to different product yields [43,44]. When using wood boards instead of powder, the heat and mass transfer phenomena within the wood board are no longer negligible. However, most of the modeling of the torrefaction process relies on the mechanisms observed in wood powder. To the best of the authors' knowledge, K impregnation in wood boards has not been done, and no

method has been established to impregnate the catalyst at an industrial scale successfully. Furthermore, since catalytic torrefaction before particle size reduction is convenient for reducing production costs, it is necessary to focus on optimizing and understanding the torrefaction of wood boards instead of powder. Therefore, this study's motivation is to propose catalytic torrefaction as the first step, followed by grinding and transportation for power/heat generation.

This study aims to scale up and investigate the feasibility of K-impregnation in wood blocks instead of powder and evaluate its impact on torrefaction. This work aims to quantify the potassium content after impregnation of wood boards having a thickness similar to what is used in industry. The purpose is to optimize wood's torrefaction duration and thermal properties and assess the effect of K-impregnation on the *TSI*. This study develops a novel insight into the relationship between K and the calorific value of the wood, which, so far, has not been established in the literature. Moreover, this work allows us to predict valuable torrefaction parameters, including *SY*, *EY*, and *EF*, based on the torrefaction duration and K content in wood using ANN. Consequently, the torrefied wood's desired solid yield and HHV can be achieved by knowing the K content and setting a convenient torrefaction duration. The results provide answers regarding the feasibility of large-scale catalytic torrefaction to upgrade biofuel and lower production costs.

Table 1
Mineral content in raw and impregnated beech.

Sample	Mineral content (wt%)					
	Mn	Mg	Са	Na	K	
Washed	0.019	0.023	0.058	0.001	0.078	
Raw	0.021	0.020	0.066	0.001	0.103	
0.004 M	0.018	0.022	0.059	0.001	0.126	
0.008 M	0.018	0.022	0.056	0.001	0.157	
0.012 M	0.014	0.018	0.068	0.001	0.207	

Table 2Potassium content and impregnation results for raw and impregnated beech wood.

K (wt%) beech powder ^a	K (wt%)	IP (%)	IR _K (%)
Not available	0.078	102.7 (5.90) ^b	-24.3
0.101	0.103	0.0	0.0
0.176	0.126	108.6 (3.75)	22.3
0.230	0.157	108.4 (5.75)	52.4
0.310	0.207	108.0 (2.95)	101.0
	Not available 0.101 0.176 0.230	Not available 0.078 0.101 0.103 0.176 0.126 0.230 0.157	Not available 0.078 102.7 (5.90) ^b 0.101 0.103 0.0 0.176 0.126 108.6 (3.75) 0.230 0.157 108.4 (5.75)

 $^{^{\}rm a}$ from a previous study using the same $\rm K_2CO_3$ solutions concentrations [65], $^{\rm b}$ Pearson standard deviation.

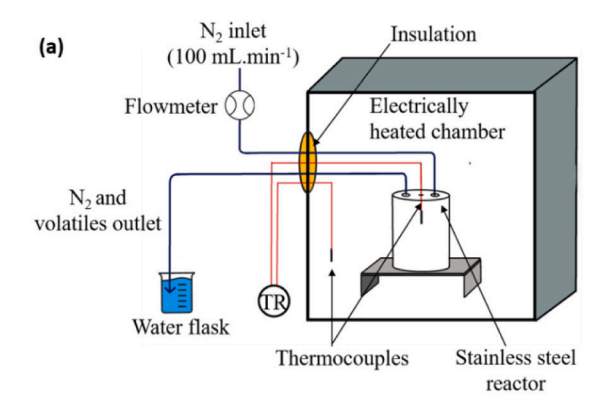




Fig. 2. (a) Wood block torrefaction device and (b) wood block before impregnation, after impregnation, and after torrefaction.

^{*}TR = temperature recorder.

^{*}TR = temperature recorder

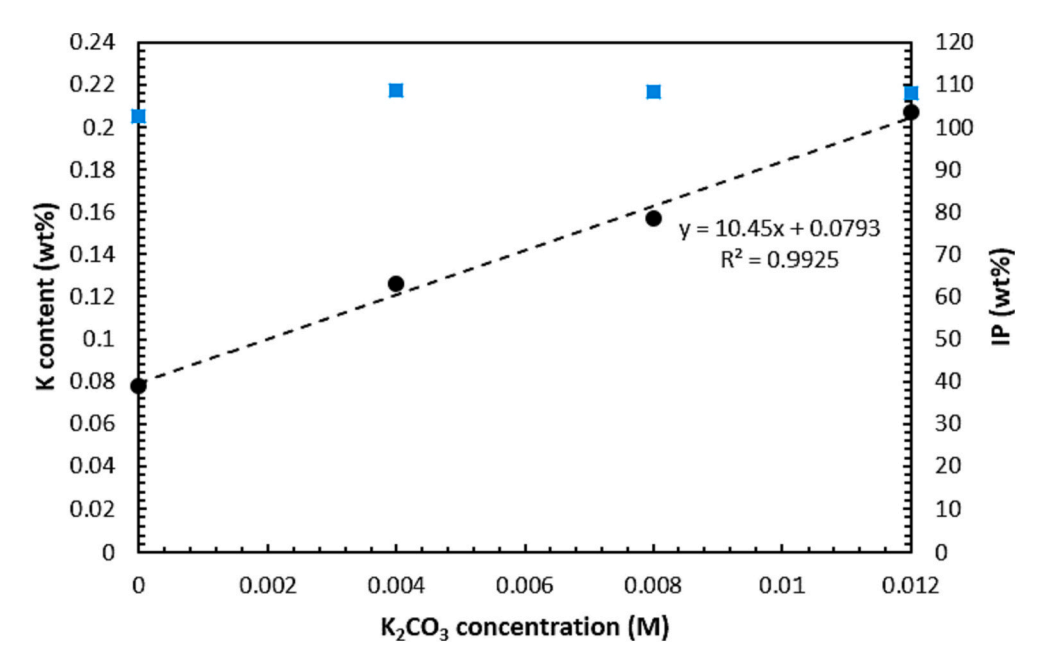


Fig. 3. Measured K content (black dots) and impregnation percentage (blue squares) in wood as a function of the K2CO3 concentration used during impregnation. (For interpretation of the references to colour in this figure legend, the reader is referred to the web version of this article.)

Table 3Beech blocks' weight loss (wt%) according to potassium content and torrefaction duration.

Sample	K (wt	Duration (min)	Duration (min)			
	%)	5	15	30	60	
Washed	0.078	26.48	31.95	38.53	51.05	
	0.078	$(1.07)^{a}$	(0.58)	(0.05)	(0.79)	
Raw	0.103	26.83 (0.37)	33.52	41.16	51.76	
	0.103	20.83 (0.37)	(1.27)	(0.31)	(80.0)	
0.004 M	0.126	29.71 (0.33)	35.20 (0.5)	43.97	53.56	
	0.120	29.71 (0.33)		(0.09)	(0.76)	
0.008 M	0.157	30.47 (0.96)	36.65	46.20	54.47	
	0.13/	30.47 (0.96)	(1.12)	(1.71)	(0.31)	
0.012 M 0.	0.207	31.92 (0.33)	37.92	49.00	56.90	
0.012 W	0.207	31.92 (0.33)	(1.82)	(1.09)	(1.02)	
$WL_{increase}$	(%) ^b	20.54	18.69	27.17	11.46	

^a Pearson standard deviation.

2. Materials and methods

2.1. Wood block impregnation and torrefaction

2.1.1. Impregnation

The selected biomass was beech wood (Fagus sylvatica), an abundant European hardwood species and easy to impregnate. Beech blocks were obtained from larger boards from France (Vosges PromoBois sawmill, in Vosges region). The wood was cut into $2\times 6\times 14~{\rm cm}^3$ (radial \times tangential \times longitudinal directions according to wood fiber orientation) blocks. The dimensions represent the industrial size and are compatible with the torrefaction reactor used in this study. The blocks were dried in an oven at 105 °C to remove moisture until mass stabilization.

Three impregnations were done using different potassium carbonate ($K_2\mathrm{CO}_3$) concentrations (0.004, 0.008, and 0.012 M), and the samples were labeled accordingly. A fourth impregnation was conducted with demineralized water only. The corresponding sample was labeled 'washed' since most water-soluble potassium was removed in the process commonly known as leaching [45]. The wood block samples were placed in a sealed tank of 10 L, filled with the impregnating solution

(Fig. 1). The impregnation was carried out using a vacuum cycle (110 mbar) for 30 min followed by a pressure cycle at 2 bars for 30 min. The impregnated blocks were air-dried for 72 h, then oven-dried at 105 $^{\circ}\text{C}$ for another 72 h.

Additional samples (raw, washed, and K-impregnated) were ground and mineralized to measure the mineral content, including potassium (K). The measurement was conducted on a dry basis (db) using atomic emission spectroscopy ICP-AES (ICP-AES 720/725 Agilent) with 200 (\pm 0.5) mg of the sample [46–48]. The impregnation percentage was calculated as the percent ratio between the increased weight of the sample compared to the dry weight [49]:

$$IP\left(\%\right) = \frac{m_{wet} - m_{dry}}{m_{dry}} \times 100\tag{1}$$

where IP is the impregnation percentage in (%), m_{wet} is the weight of the wet sample immediately after impregnation (g), and m_{dry} is the dry weight of the sample before impregnation (g). The impregnation ratio of K (IR_K) is the percentage of addition or removal of potassium relative to the content present in the raw wood calculated as:

$$IR_{K}\left(\%\right) = \frac{K_{i} - K_{raw}}{K_{row}} \times 100 \tag{2}$$

where K_{raw} and K_i are the potassium contents in the raw and impregnated samples (i = washed, 0.004 M, 0.008 M, or 0.012 M), respectively.

2.1.2. Pilot-scale torrefaction

The dry-impregnated samples were placed in a cylindrical stainless-steel reactor (Fig. 2.a). The reactor had a gas inlet to keep the atmosphere inert using 100 mL.min^{-1} of nitrogen (N₂) and an outlet linked to a water trap to remove condensables and tars. The reactor was placed inside a heating chamber equipped with a fan that homogenizes the heat flow across the reactor. Each sample was loaded in the sealed reactor and heated from room temperature to 300°C at a heating rate of $2\,^{\circ}\text{C}$. min^{-1} . The chosen heating rate is close to the ones used in industrial torrefaction facilities [44]. The temperature was then held at 300°C for four torrefaction durations of 5 min, 15 min, 30 min, and 60 min.

The sample was weighed before and after torrefaction using an *OHAUS Analytical Plus* balance (precision 0.1 mg). The weight loss was calculated as $WL = \frac{m_0 - m_f}{m_0} \times 100$; where WL is the weight loss (wt%), m_0

^b WL_{increase} = 100 × (WL_{0.012 M} - WL_{Washed})/WL_{Washed}.

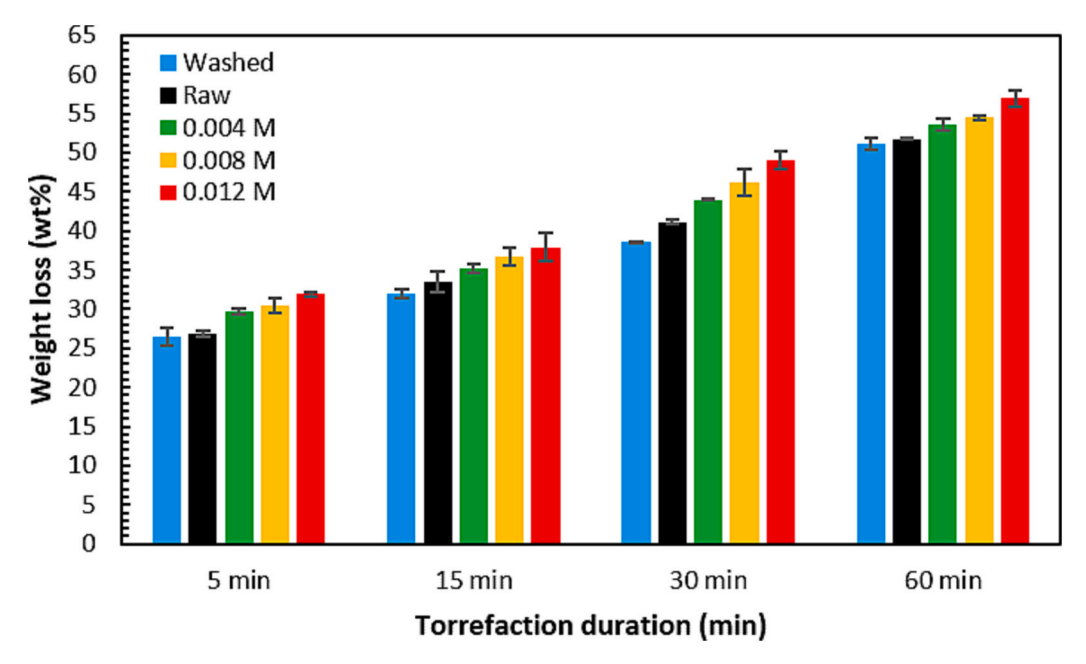


Fig. 4. Weight loss evolution (with the standard deviations) of wood blocks after the different torrefaction durations.

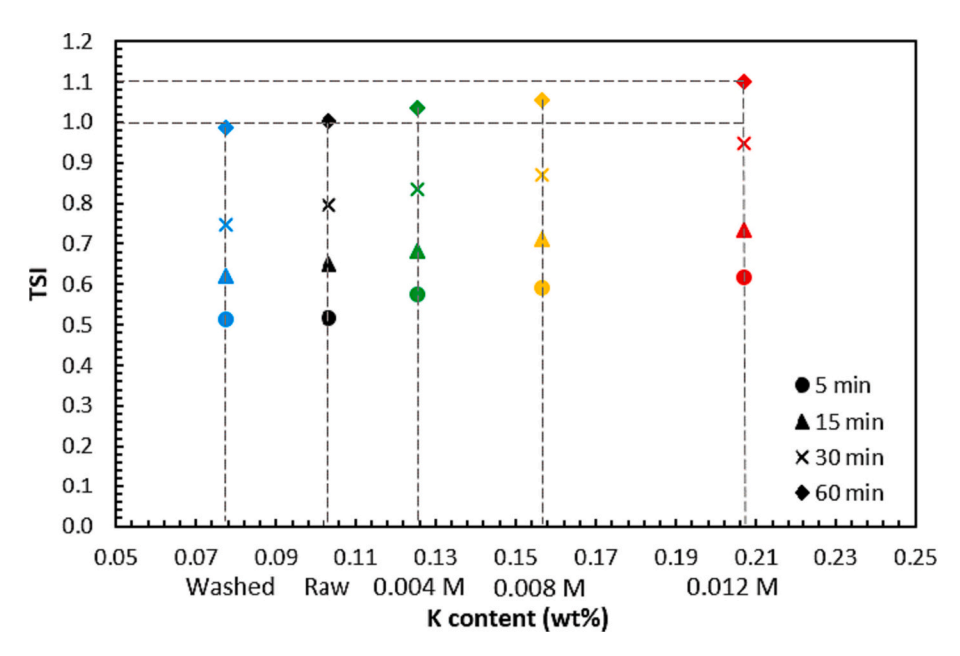


Fig. 5. TSI in the function of potassium content in the sample for the different torrefaction durations.

is the dry weight of wood before thermal treatment (g, dry-basis), and m_f is the wood's weight after torrefaction (g, dry-basis). Moreover, each experiment was done in triplicate and represented along with the standard deviation of the weight loss defined as: $\sigma = \sqrt{\frac{\sum (WL - WL_{uv})2}{n}}$. σ is the standard deviation (wt%), WL_{uv} is the average weight loss (wt%), and n is the number of trials (i.e., n=3 in this case).

2.2. Torrefaction performance

2.2.1. Torrefaction severity index (TSI)

TSI is an efficient indicator of the torrefied biomass quality [50]. Being normalized based on the weight loss at 300 $^{\circ}$ C for 60 min, it considers the two most influential parameters in torrefaction: temperature and duration, independently of the biomass species. The TSI was

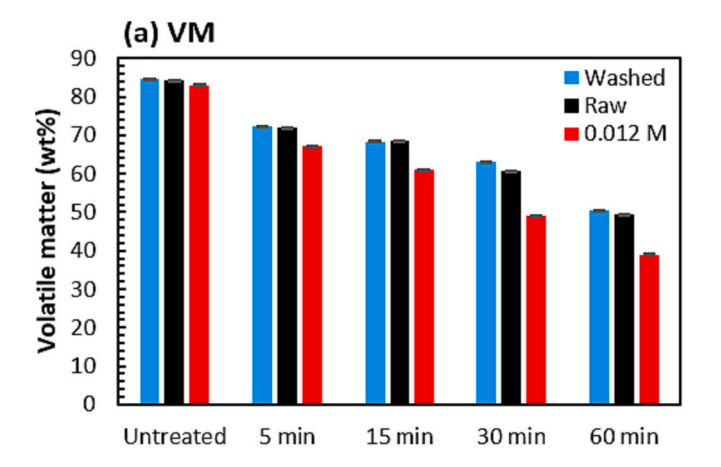
calculated according to Eq. 3 [7]:

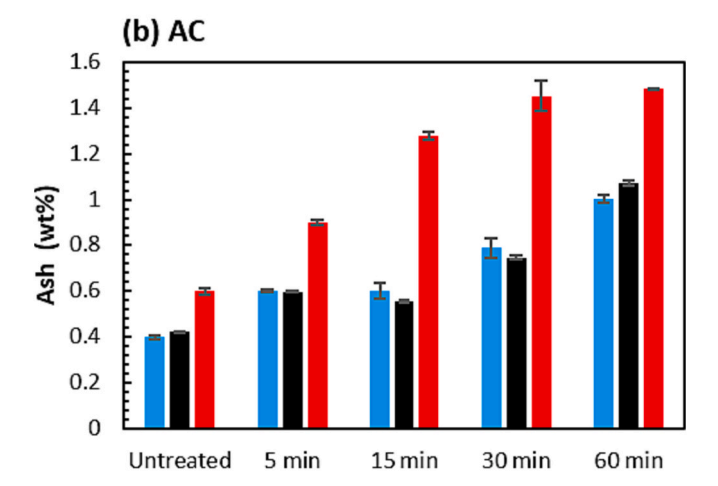
$$TSI = \frac{WL_{T,t}}{WL_{300^{\circ}C,60 \text{ min}}} \tag{3}$$

where $WL_{T,t}$ is the weight loss (wt%) at a certain torrefaction temperature (T in °C) and time (t in min) and $WL_{300^{\circ}C,60~min}$ is the weight loss of raw wood block after 60 min torrefaction at 300 °C.

2.2.2. Proximate and elemental analysis

The proximate analysis gives information about the ash (AC), volatile matter (VM), and fixed carbon (FC) contents in wt% of a sample. It is linked to a solid fuel's combustion properties [51]. The analysis was performed according to ISO procedures: ISO-18122 (AC) [52] and ISO-18123 (VM) [53], and the difference corresponds to FC (FC = 100 - (AC + VM)). The AC and VM determinations were performed using an





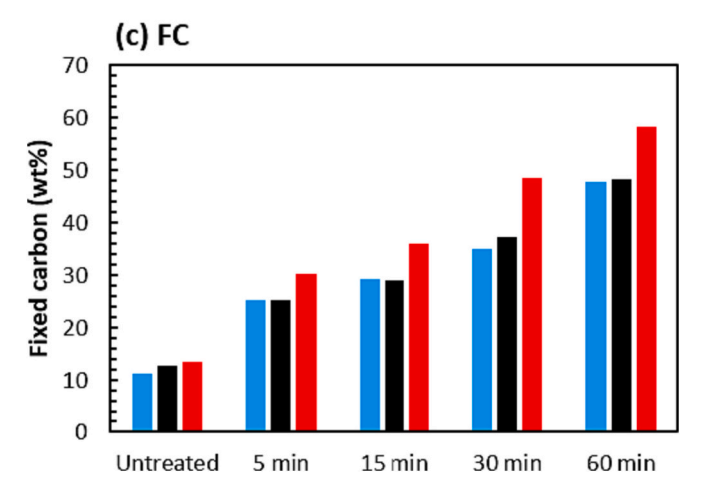


Fig. 6. Proximate analysis with standard deviation of untreated and torrefied woods at different durations and K concentrations.

OHAUS Analytical Plus balance and a muffle furnace Carbolite CSF 1200. The standard deviation was calculated for the AC and VM. The FC was represented without standard deviation since it was obtained by difference. The elemental analysis was determined using a CHNS analyzer (Thermo Scientific FlashSmart Elemental Analyzer). It determines the carbon (C) and hydrogen (H) percentages in the sample, and the oxygen (O) was obtained by subtraction (%O = 100 - (%H + %C)). The atomic ratios H/C and O/C were calculated and represented in the van Krevelen diagram, in which a lower ratio indicates a higher fuel energy content [54]. The data ranges of biomass, peat, lignite, coal, and anthracite in

the van Krevelen plot were taken from the literature [55].

2.2.3. Energy analysis

The higher heating value (*HHV*) characterizes a fuel's gross energy during combustion [56]. It was measured according to ISO-18125 [57] using a *Parr 6100 Calorimeter*. The calorimeter bomb was filled with pure oxygen to obtain complete combustion of the sample. Dry untreated and torrefied beech samples (raw, washed, and K-impregnated) were ground and then pressed into 0.5 g pellets. The pellet was linked to the ignition thread and loaded inside the bomb vessel of the calorimeter. The sample was burned, and the calorimeter computed the produced energy per unit of mass of the sample. The experiments were performed in duplicates, and the mean values were used since the relative error was below 3%.

The energy yield (EY) is a significant index for measuring the torrefaction performance, while the enhancement factor of the HHV (EF) evaluates the torrefaction quality [58]. The EY and EF are related through the solid yield (SY), which is the weight ratio of torrefied biomass to the raw one. The SY, EF, and EY were calculated according to Eqs. 4–6 [59]:

$$SY\left(\%\right) = \frac{m_{torrefied}}{m_{raw,untreated}} \times 100\tag{4}$$

$$EF = \frac{HHV_{torrefied}}{HHV_{raw,untreated}} \tag{5}$$

$$EY\left(\%\right) = EF \times SY\tag{6}$$

where $m_{torrefied}$ and $m_{raw,untreated}$ are respectively the weight of the torrefied sample (having different K content) and raw sample without torrefaction (g, dry-basis). $HHV_{torrefied}$ and $HHV_{raw,untreated}$ are the higher heating values of the torrefied sample (having different K contents) and raw sample without torrefaction (g, dry-basis). Then the relative solid yield (RSY), relative energy yield (REY), and relative enhancement factor (REF) were calculated as $RX_{i,j}/RX_{raw,j}$. X is the SY, EY, or EF, i is the sample (washed, raw, 0.004, 0.008, or 0.012 M), and j is the torrefaction duration (5, 15, 30, or 60 min).

2.3. Machine learning

Machine learning consists of training the machine learning model until it can efficiently optimize the output based on some changes in the input data [37]. In this study, ANN is selected to predict the torrefaction behavior using Megaputer PolyAnalyst 6.5. This is represented by the prediction of the three important biofuel outputs: EY, SY, and EF. The input parameters were the K content and torrefaction duration. The data were divided into 70% for training and 30% for testing according to what is recommended in the literature for biomass torrefaction [60]. Then different combinations of activation functions (Sigmoid, Elliot, and Piecewise linear) and learning methods (Quick propagation, Backpropagation, and RPROP) were tested to obtain the highest efficiency [38]. The neuron number in the hidden layer was obtained according to the method used by Aniza et al. [38]. It equals powers zero to three of the input variables (2 input types in this case), resulting in 1, 2, 4, and 8 neurons tested (i.e., $8 = 2^3$). Once the model is trained, it can predict the EY, SY, and EF based on different inputs. Then the relative error between experimental data and estimated values was calculated to evaluate the ability of the ANN to predict the torrefaction behavior.

3. Results and discussion

3.1. Impregnation efficiency

The results of ICP-AES concerning the five most abundant minerals in wood are shown in Table 1. Among the five minerals of Mn, Mg, Ca, Na, and K, potassium's yield was the highest (0.103 wt%) and sodium was

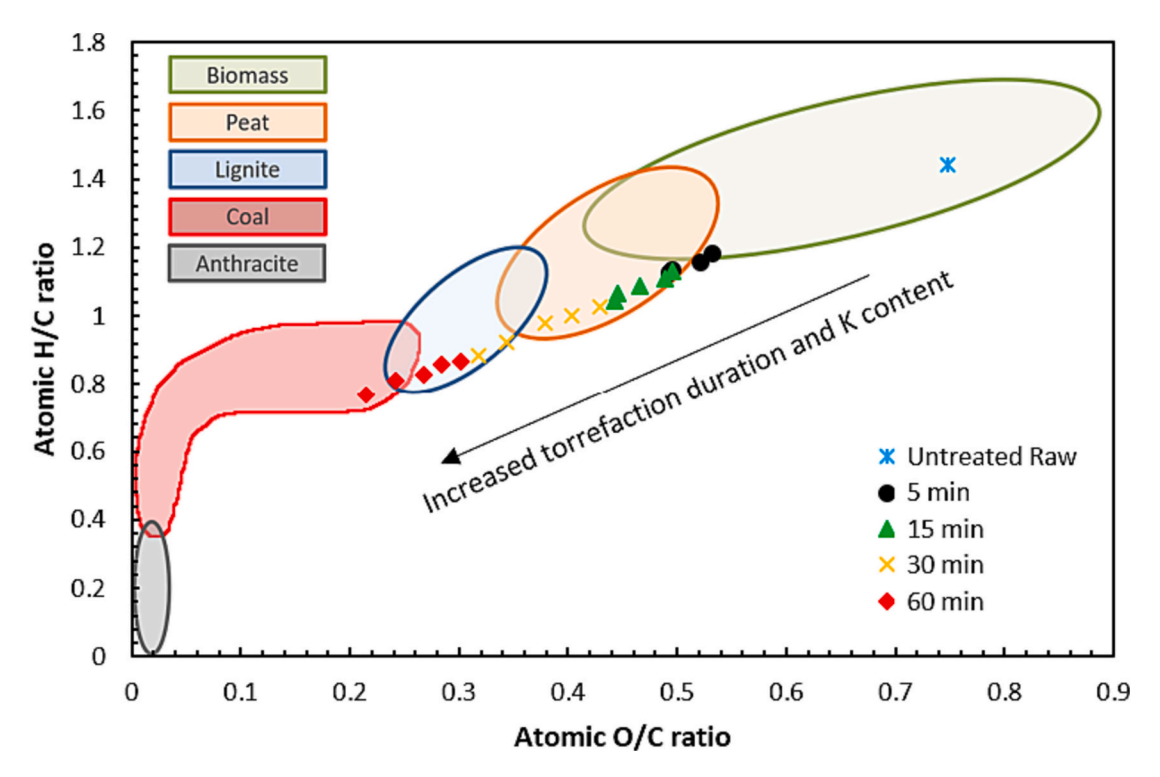


Fig. 7. Van Krevelen diagram of untreated and torrefied woods having different K concentrations.

the lowest (0.001 wt%) [61,62]. The mineral content (Mn, Mg, Ca, and Na) remained almost constant after the impregnations. The only one that varied with the different impregnations was the potassium content which decreased with the washing and increased with the addition of K_2CO_3 solution [63].

The impregnation results are presented in Table 2. The IP was above 100%, meaning that the impregnation cycle applied (30 min vacuum +30 min pressure) was sufficient for the wood to absorb the impregnation solution. The vacuum cycle frees the air trapped in the wood to allow for the impregnating solution to penetrate. Then, increasing the pressure improves the permeability, but high pressure could alter the wood's physical or chemical properties [49,64]. The potassium impregnation ratio (IR_K) ranged from -24.2% to 101.0% between the washed and 0.012 M solution. This means that the demineralized water impregnation removed 24.3% of the K present in the wood, while the impregnation with 0.012 M of K_2CO_3 doubled the K content (0.207 wt%) compared to the raw (0.103 wt%).

The evolution of the K content in wood measured by the ICP-AES in the function of the molarity of the impregnating solution of $K_2 CO_3$ was plotted in Fig. 3. The increase of K content in wood increased linearly with the $K_2 CO_3$ solution concentration ($R^2=0.9925$). Therefore, for beech wood, the linear equation could be used in this range to predict the actual K content based on the solution prepared. The highest concentration added (0.012 M) did not saturate the wood with K; therefore, higher concentrations could potentially be used for impregnation.

A previous study was conducted on wood powder using the same concentrations of K_2CO_3 solutions [65]. The ICP-AES results are also presented in Table 2. They show that the efficiency of wood powder impregnation was close to the block for 0.004 M. This K content increased more rapidly in powder with the increase of K_2CO_3 concentrations. This behavior is expected, considering that wood is a porous material, and the thicker the sample, the more difficult it is for K to diffuse [66]. Moreover, when impregnating wood powder, the contact surface between the impregnation solution and the wood is larger than the wood block.

3.2. Torrefaction performance

3.2.1. Weight loss and TSI

The weight loss of wood at the four torrefaction durations was represented in Table 3 and plotted in Fig. 4. The weight loss, ranging from 26.48 to 56.90 wt%, increased with increasing torrefaction time and K content. Based on the literature, a weight loss of beech wood ranging from 30 to 48 wt% is required to reach moderate to very good grindability [67]. Thus, impregnating wood blocks with potassium followed by a torrefaction could be a cost-effective pretreatment method for wood used in energy production. Moreover, the weight loss of the 0.012 M wood block after 5 min torrefaction (31.92 wt%) was equal to that of the washed block after 15 min torrefaction (31.95 wt%). The same behavior could be observed between 0.012 M beech torrefied for 15 min (37.92 wt%) and the washed torrefied for 30 min (38.53 wt%). These results prove that adding K to the wood reduced the torrefaction duration by up to 67%. Safar et al. [68] reported a similar behavior for wood powder impregnated with the same concentrations of K2CO3 and torrefied at 300 °C. They found that to achieve a weight loss of 40 wt%, K-impregnation can reduce the torrefaction duration by 28%. In this study on wood boards, to achieve a similar weight loss (approximately 39 wt%), 50% of the torrefaction duration can be gained instead of 28%. Consequently, the scale-up from wood powder to wood boards was highly efficient in terms of operating time reduction. The results can be explained by the scale change from powder to wood boards, where the produced volatiles inside the board have more difficulty evacuating to the atmosphere. These volatiles include some catalytic by-products, such as acetic acid, that can further react to degrade the wood due to longer residence time [69]. Additionally, exothermic reactions have been observed with increasing the wood's thickness [44], which could be enhanced in the presence of potassium, resulting in a more substantial catalytic effect.

The relative weight loss increase between the 0.012 M sample and the washed was almost constant, ranging between 20.54% and 18.69%, respectively, after 5 min and 15 min torrefaction. As the torrefaction duration was prolonged to 30 min, the catalyzing impact of K was accentuated, reaching up to 27.17% of weight loss increase with 0.012

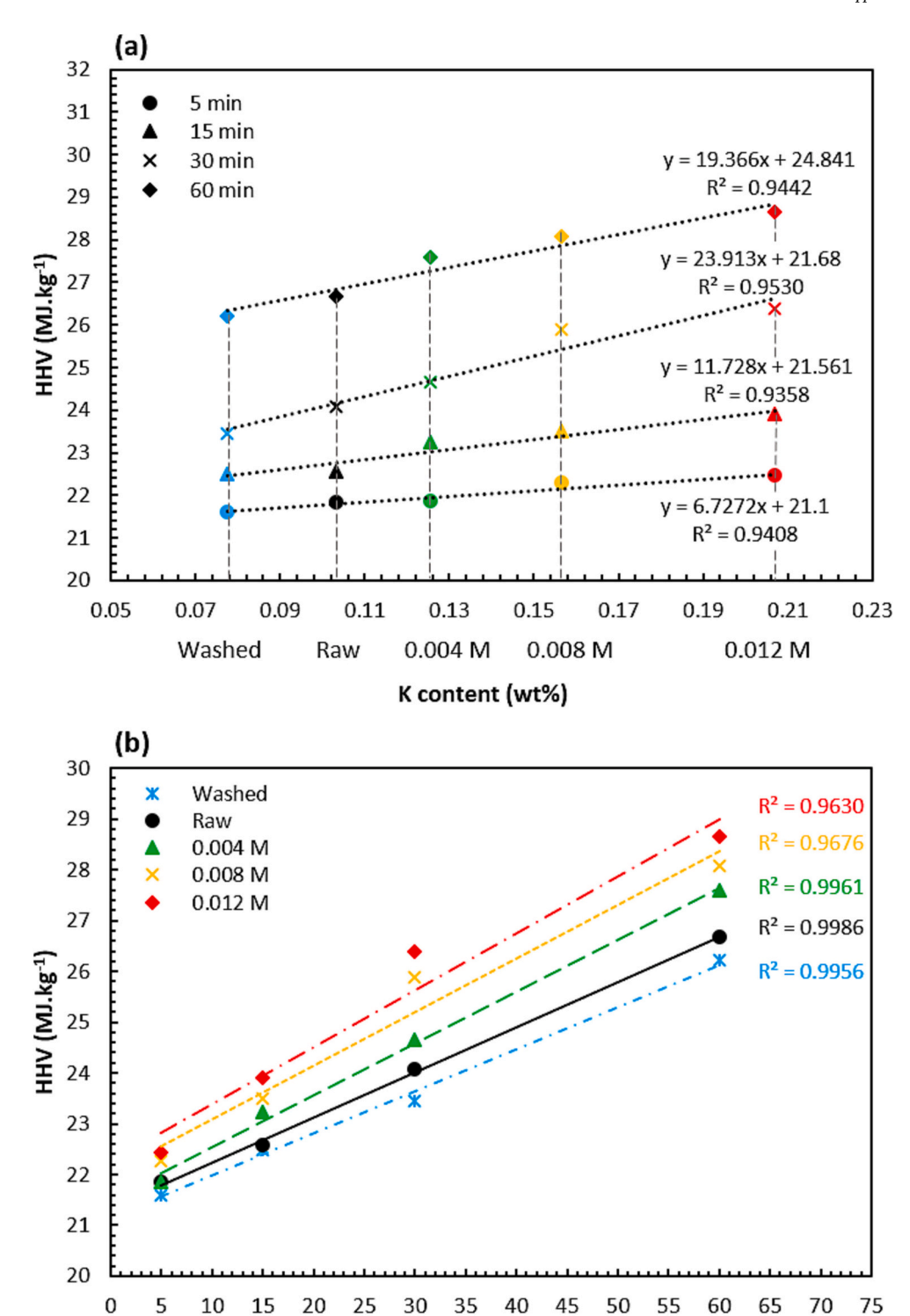


Fig. 8. HHV (a) versus potassium content in sample and HHV (b) versus the torrefaction duration.

Torrefaction duration (min)

M compared to the washed. After 60 min torrefaction, the degrading effect of potassium dropped quickly (11.46%) with a weight loss of 56.9 wt% for the 0.012 M. This weight loss could correspond to the point where the hemicelluloses and most of the cellulose have been degraded, thus approaching the limit of the potassium's catalyzing effect on wood's thermal degradation [42,63]. This behavior was demonstrated in a previous study [65] on wood powder doped with different K concentrations: during torrefaction at 300 $^{\circ}$ C, the weight loss increased for the samples with a higher K content. But as the weight loss approached

65 wt%, the catalytic effect of potassium started to decrease. After this point, potassium promoted char formation instead of wood degradation. In the case of wood blocks, this behavior can also be observed. The decrease of the catalytic efficiency of K between 30 min and 60 min is probably also due to the weight loss getting close to 65 wt%. This could be attributed to the fact that potassium primarily acts on celluloses and hemicelluloses [42]. As the torrefaction extent increases, these components are almost completely degraded.

Although not fully elucidated due to its great complexity, it is

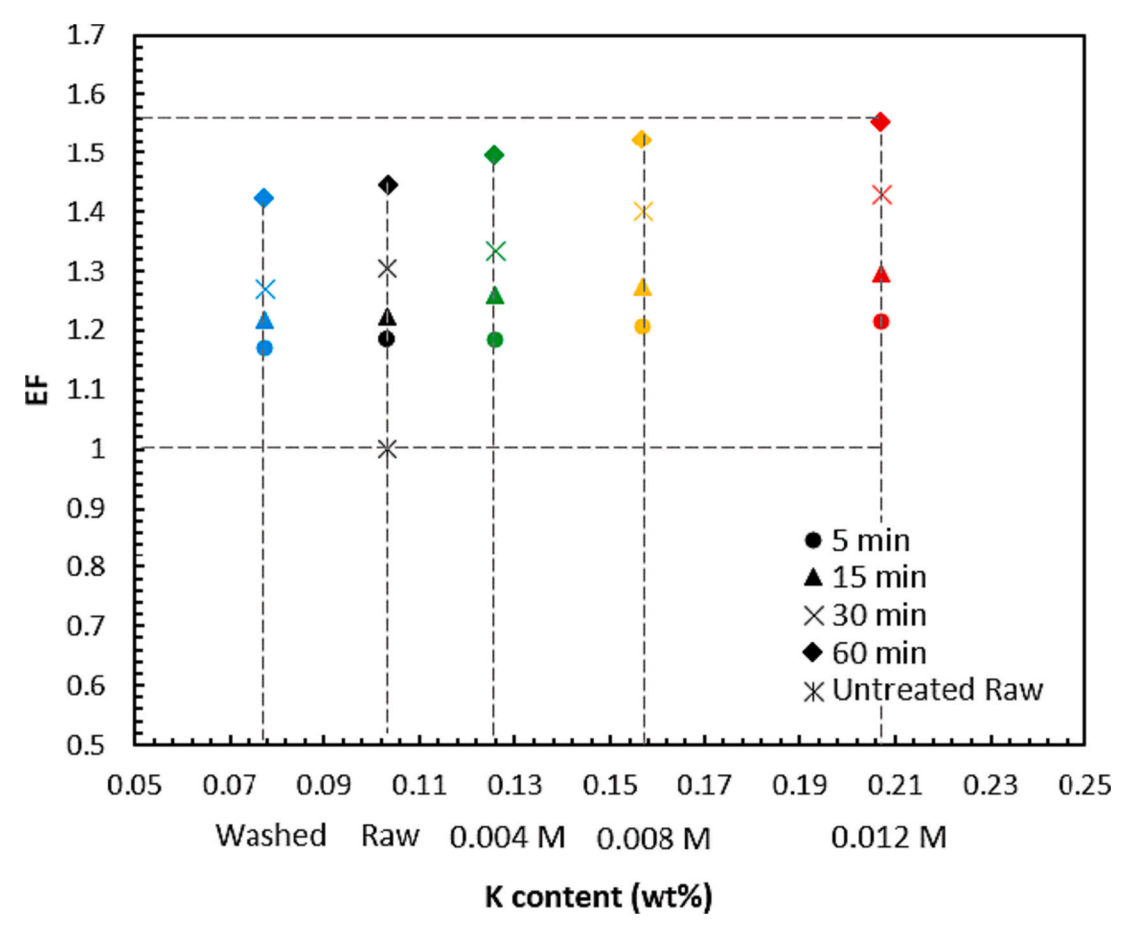


Fig. 9. EF of HHV relative to untreated raw beech versus potassium content in sample.

Table 4 Calculated *SY*, *EY*, and *EF* for the different wood samples.

	Washed	Raw	0.004 M	0.008 M	0.012 M
5 min					
SY (%)	73.52	73.17	70.29	69.53	68.08
EY (%)	86.06	86.60	84.65	83.80	82.83
<i>EF</i> (-)	1.17	1.18	1.18	1.21	1.22
15 min					
SY	68.05	66.48	64.80	63.35	62.08
EY	82.90	81.31	81.57	80.63	80.42
EF	1.22	1.22	1.26	1.27	1.30
30 min					
SY	61.52	59.69	56.98	52.09	51.00
EY	78.16	77.88	76.08	73.05	72.92
EF	1.27	1.30	1.34	1.40	1.43
60 min					
SY	48.95	48.24	46.44	45.53	43.10
EY	69.52	69.73	69.42	69.27	66.92
EF	1.42	1.45	1.49	1.52	1.55

believed that the mechanism driving the torrefaction of wood consists of an intricate combination of chemical transformations involving the main wood constituents (cellulose, hemicelluloses, and lignin), extractives, and their thermal degradation by-products. Many studies have revealed the formation of CO_2 , water, and acetic acid among the main products obtained during torrefaction [70]. Hydrolysis of polysaccharides (such as cellulose and hemicelluloses) is known to take place under acidic conditions. The partial degradation of relatively chemically

active hemicelluloses and amorphous cellulose improves material properties. Previous studies suggested that K^+ ions assist in transforming the cellulose molecules' structure from crystalline to amorphous by weakening hydrogen bonds [32]. The results reported herein indicate that K^+ directly affects wood torrefaction, accelerating thermal degradation. It can be speculated that K^+ can work as a Lewis acid, interacting directly with electron-rich sites along the wood structure, most likely increasing the polarity of glycosidic bonds in cellulose and hemicelluloses, leading to easier hydrolysis in comparison to torrefaction performed in the absence of $K_2\text{CO}_3$ impregnation.

The TSI (Fig. 5) increased as a function of the wood's torrefaction duration and potassium content [71]. The extent of the torrefaction was improved in the samples doped with potassium, reaching a TSI of 1.10. This value was higher than the maximum expected TSI as it is a normalized index between 0 and 1 [72]. For example, the torrefaction severity index was enhanced by 10% when torrefaction was operated at 300 °C for 60 min torrefaction with the impregnation of 0.012 M K_2CO_3 . A higher TSI is associated with better biochar quality [50,73].

3.2.2. Proximate analysis

Proximate analysis is important for biochar characterization because it is inexpensive to test the fuel's quality. The AC, VM, and FC of the washed, raw, and 0.012 M samples were plotted for the different torrefaction experiments (Fig. 6). A low VM is an indicator of a higher coal rank because it significantly impacts the presence or absence of complete combustion at low temperatures [74]. This study showed a strong decrease of the VM by 54%, reaching 39.0% for the 0.012 M wood torrefied for 60 min. Lower VM in biomass is desired because it lowers GHG emissions during combustion due to decreased $\rm CO_2$ production [75]. The ash content increased in the wood blocks that were previously

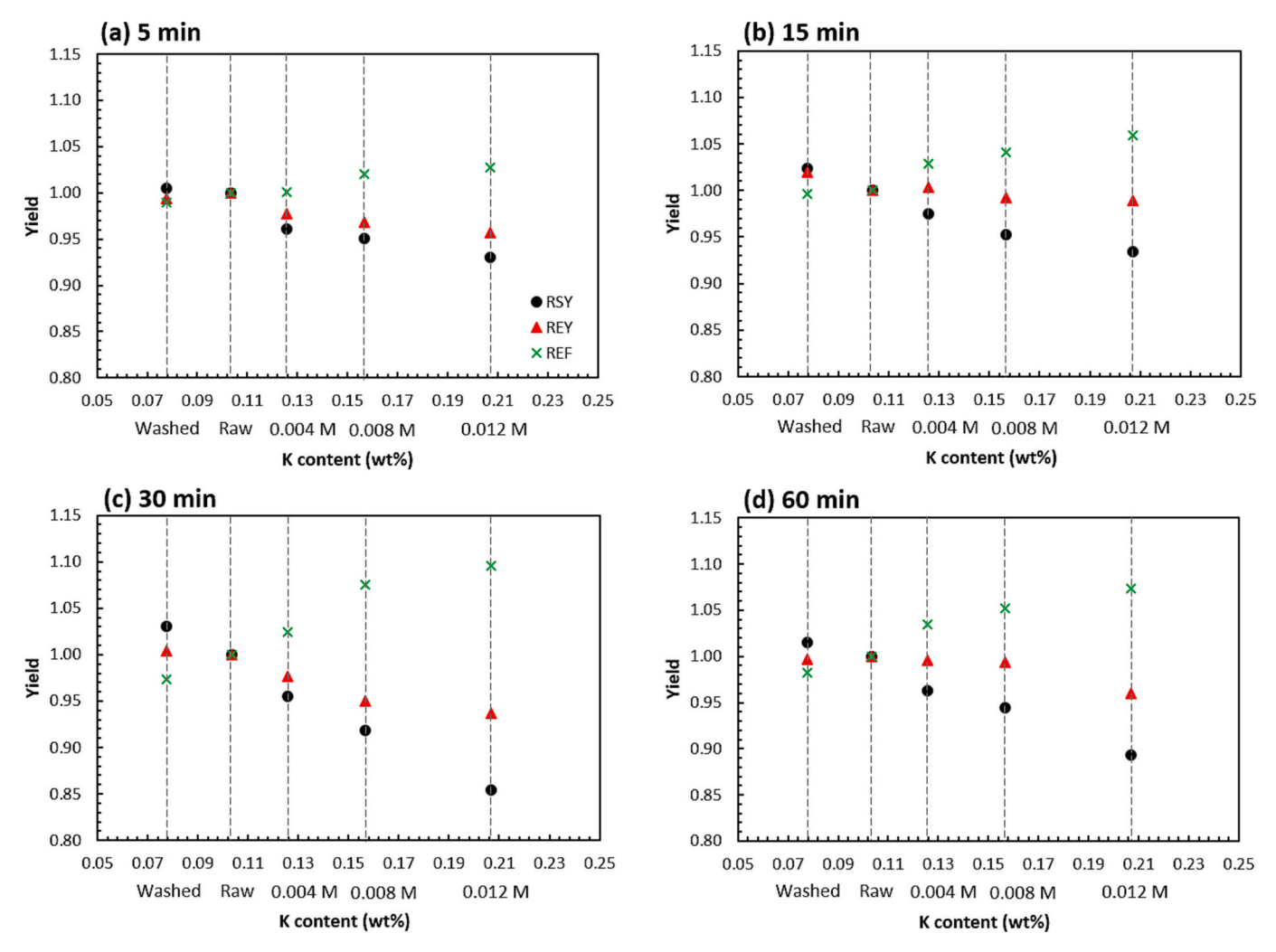


Fig. 10. REY, RSY, and REF variation with potassium content in sample for the different torrefaction durations (a) 5 min, (b) 15 min, (c) 30 min and (d) 60 min.

Table 5ANN training results for *SY*, *EF*, and *EY* prediction.

Test	Neurons	Hidden layer	Outut layer	Training	R ² EY	R ² EF	R ² SY
1	1	Elliot	Piecewise	Quick	0.9306	0.9047	0.9173
2	1	Sigmoid	Elliot	Back	0.7658	0.8384	0.8910
3	1	Elliot	Piecewise	RPROP	0.9413	0.9080	0.9339
4	2	Piecewise	Elliot	RPROP	0.7836	0.8144	0.4821
5	2	Sigmoid	Piecewise	Quick	0.9750	0.9308	0.9266
6	2	Elliot	Sigmoid	Back	0.8328	0.9796	0.9811
7	4	Elliot	Piecewise	Back	0.9913	0.9948	0.9444
8	4	Sigmoid	Elliot	Quick	0.7867	0.8346	0.7307
9	4	Piecewise	Sigmoid	RPROP	0.5321	0.5985	0.4351
10	8	Sigmoid	Piecewise	RPROP	0.9922	0.9991	0.9986
11	8	Piecewise	Elliot	Back	0.7649	0.8131	0.7471
12	8	Elliot	Sigmoid	RPROP	0.9989	0.9997	0.9991

torrefied and was even higher for the K-impregnated sample. This could be partially attributed to the higher potassium content in the impregnated and torrefied wood that probably remained in the ash upon combustion at 550 °C [45,76]. Additionally, as the potassium intensified the wood's degradation, it led to a lower VM, resulting in relatively more ash. Despite the increased AC, the value ranging from 0.41% to 1.48% is low compared to most coals' AC, which varies between 0 and 70% [77]. After K-impregnation and 60 min torrefaction, the FC registered an increase of >5 times compared to the washed untreated wood, reaching 58.4%. The potassium had a visible effect on the rise of the FC, especially for the longer torrefaction durations. A higher FC content leads to a

higher combustion quality and thus makes the torrefied K-impregnated biomass more suitable as a fuel source [78]. As one of the technical issues of biomass in co-combustion is its high VM and low FC, using this approach allows shifting these proportions for energy production and increases the process efficiency [7].

3.2.3. Atomic H/C and O/C ratio

The van Krevelen diagram (Fig. 7) demonstrated the effect of torrefaction duration and increasing K content in wood on the atomic O/C and H/C ratios. The two ratios decreased drastically as the torrefaction severity (e.g., duration or K content) increased. They shifted from the

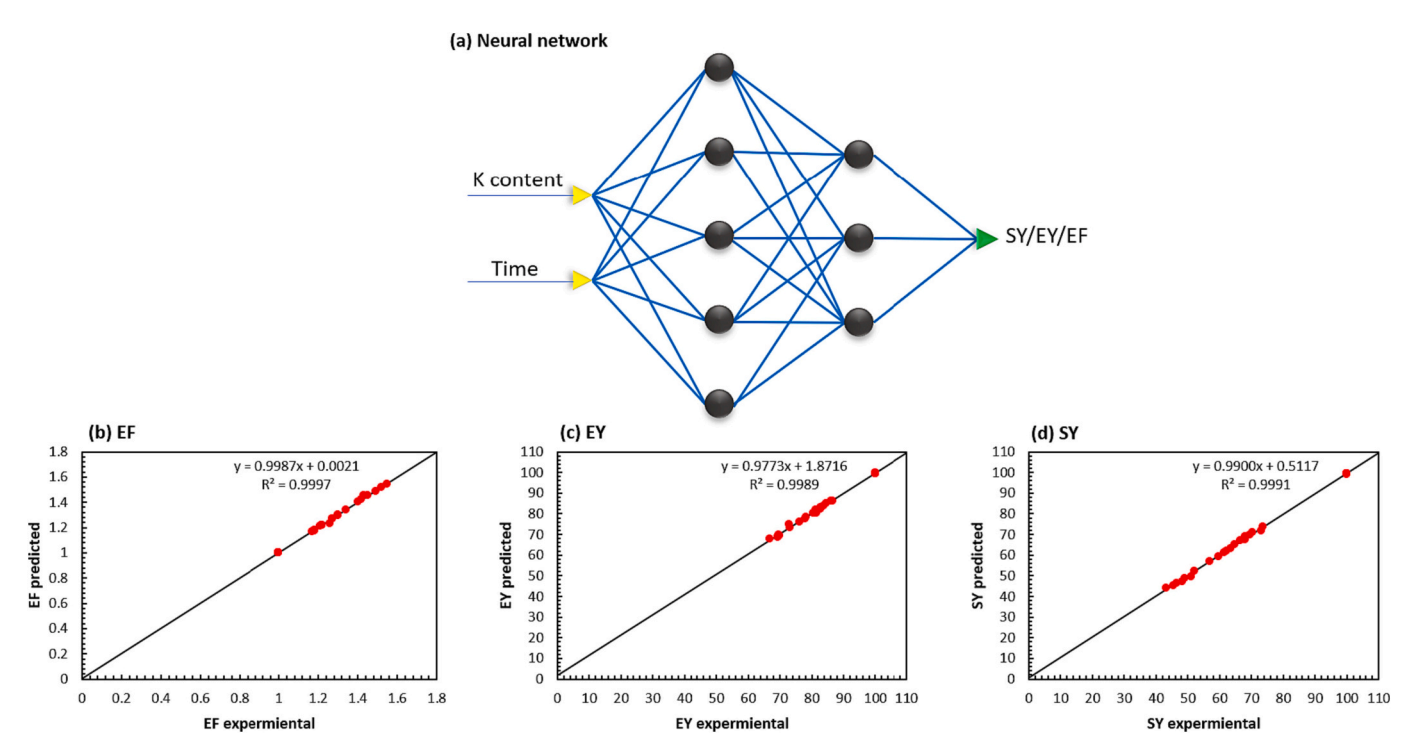


Fig. 11. (a) Neural network structure with highest fit quality R², and (b-d) the predicted ANN results as a function of the experimental data.

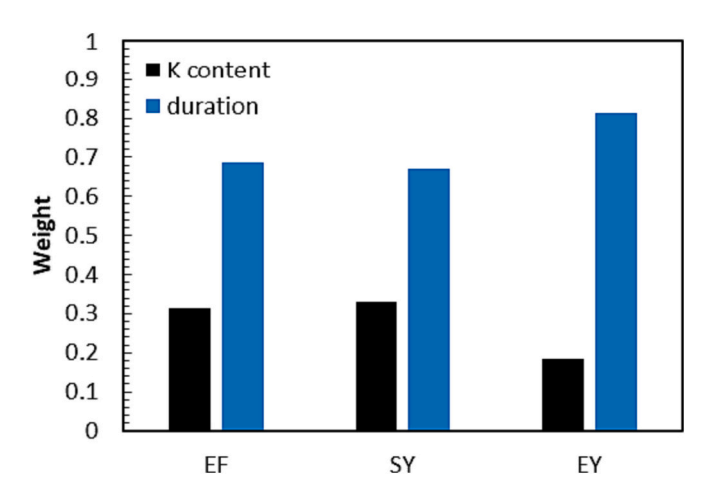


Fig. 12. Weight of the inputs (K content and torrefaction duration) that influences each of the SY, EY, and EF.

biomass range (untreated raw wood) to the coal range for the 0.008 M and 0.012 M samples at 60 min torrefaction. Additionally, the 0.012 M sample torrefied for 60 min was close to meeting the criteria of the European biochar certificate, where biochar evaluated is often obtained from biomass pyrolysis. Therefore, this catalytic torrefaction at 300 °C achieved results expected to be obtained at a higher temperature range. The 0.012 M sample's carbon yield was above 50 wt% db, and the O/C was below 0.4. However, the H/C reached 0.76, higher than the required value of 0.7 [79]. It should be noted that the lower the O/C and H/C ratios, the higher the coal rank [80]. Furthermore, the achieved low O/C ratio is desirable in gasification to limit exergetic losses [81,82], which makes this proposed torrefaction process a viable pretreatment for multiple uses, including biomass gasification.

3.2.4. Higher heating value

A linear relationship between *HHV* increase and weight loss increase during torrefaction has been studied in the literature [83–85]. However,

the linear profile of HHV with increasing K content or torrefaction duration has not been reported yet. The increased potassium content in wood (Fig. 8a) and the longer torrefaction duration (Fig. 8b) positively impacted the wood blocks' HHV. Specifically, Fig. 8a shows a linear correlation between the HHV and the potassium content in wood (0.94 $< R^2 < 0.95$), and Fig. 8b depicts a higher linear correlation between the $\it HHV$ and torrefaction duration (0.96 < $\it R^2$ < 1). The $\it HHV$ of torrefied wood varied between 21.59 MJ.kg⁻¹ for washed sample (5 min) and a maximum of 28.65 MJ.kg⁻¹ for the 0.012 M sample (60 min). This maximal value was higher than that of low-rank coals, typically between 21 and 22.7 MJ.kg⁻¹, and was close to that of bituminous coal commonly used for power generation (24.4–32.6 MJ.kg⁻¹) [86–88]. Biomass needs to have a higher energy density to achieve boiler load stability; therefore, coal-like properties are important for co-firing with coal [17]. Tumuluru et al. [89] stated that for co-firing biomass and coal, biomass requires a higher heating value, higher storage stability, and lower moisture content that can be achieved through torrefaction.

Fig. 9 represents the EF of the HHV of all samples (torrefied and nontorrefied, K-impregnated and unimpregnated) relative to the HHV of untreated raw beech (18.45 MJ.kg⁻¹). The torrefaction increased the HHV between 18% and 45% for the wood torrefied between 5 min and 60 min. The effect of torrefaction on the HHV of biochar was consistent with the literature [90,91] and with the atomic H/C and O/C ratios obtained (part 3.2.3) [7,92]. Moreover, the potassium further increased the HHV by 55% (EF = 1.55) after 60 min torrefaction for the 0.012 M sample. The increased HHV with the K-impregnation was reported in the literature for the biodiesel and biochar produced from beech wood pyrolysis [88]. However, no studies in the literature were made to relate the impact of K on the improvement of HHV during torrefaction. The increase observed in this study is attributed to the improved weight loss through the degradation of celluloses and hemicellulose, which mainly leaves a relatively larger lignin content with a higher HHV (23.3-26.6 $MJ.kg^{-1}$) [7,94].

3.2.5. Relative energy yield

The computed SY, EF, and EY for the different conditions used are presented in Table 4. Based on the literature, an energy yield of around

80% is considered good, mainly when associated with a high EF [72]. The energy yield was above 80% for all samples torrefied for 15 min at 300 °C with a solid yield between 68.05 and 62.08%. These results agree with the study of Peng et al. [95], which found an EY of 80% for an SY of 70%. For longer durations, the EY decreased faster but was still related to a continuous increase of the EF until 1.55.

The *REY*, *RSY*, and *REF* were plotted in Fig. 10 to understand more profoundly the impact of the K and torrefaction duration on these thermal parameters. The results confirmed that with the increase of torrefaction severity (duration and K content), the *REF* increased but led to declined energy efficiency. The highest difference was observed for the 0.012 M sample after 30 min torrefaction marked by a *REY* (0.94), almost equal to 0.008 M, and had the highest increase of the *REF* of 1.10. A compromise should be found between the allowable reduction of the energy yield (the energy retained by the wood after thermal treatment) and the improvement of the *EF* [90]. Therefore, a less severe treatment should be investigated for industrial applications by reducing the treatment duration or temperature.

3.3. Artificial neural network prediction

The ANN training results are shown in Table 5. The highest fit quality R^2 for the SY (0.9991), EY (0.9989), and EF of the HHV (0.9997) was obtained using 8 neurons constructed according to Fig. 11a. Excellent results were achieved using Elliot function in the hidden layer, Sigmoid in the output layer with RPROP training method. Onsree et al. [97] used gradient tree boosting machine learning to predict the SY of torrefied biomass and obtained a fit quality R² equal to 0.90. The results obtained in this study with $R^2 > 0.99$ suggest that ANN is more robust for predicting the catalytic torrefaction performance. The predicted results were validated in Fig. 11b. The linearity analysis shows excellent fit quality between the predicted and experimental results for all parameters (SY, EY, and EF). The supervised ANN models that yielded the highest R² were tested for combinations of K content and torrefaction durations and yielded results with a relative error below 3%. These findings can target specific results, such as the SY, by evaluating different combinations of the input parameters [38]. The ANN model has robust predictions according to the tested range and conditions. For more general applications in the industry, more data should be fed to the model to account for larger variations in the conditions or even the different biomass species. Upon sufficient training, the ANN has a promising potential to optimize the catalytic torrefaction process according to the desired product characteristics (EY, SY, or EF).

Fig. 12 shows the influence weight of each variable on the torrefaction's outcome. The K content's influence on the EF and SY was not negligible, with a weight of 0.313 and 0.329, respectively. This highlights potassium's influence on HHV improvement and weight loss during torrefaction. However, the torrefaction duration largely impacted EY with a weight of 0.814. This correlates with the literature that found the torrefaction time to have the most effect (second to temperature) on the EY of torrefied biomass [7,98]. By further developing these findings, they may be integrated into the management and optimization of ANN-assisted bioenergy systems in industry and research technology.

4. Conclusions

The tested impregnation method on wood blocks led to a linear increase of the K content diffused in wood in regards to the molarity of the impregnation solution. Additionally, by changing the scale and performing the catalytic torrefaction on wood boards, the catalytic effect of potassium gave better results than what was reported for wood powder. The torrefaction duration was reduced by up to 67% with K addition. Moreover, increasing the potassium content in wood increased the severity of torrefaction to achieve a *TSI* up to 1.10. The K-impregnated torrefied wood had a lower VM and higher FC, corresponding to

upgraded fuel properties. Moreover, the relative H/C and O/C ratios decreased, and the HHV reached values comparable to coal. A linear increase of the HHV with the torrefaction time and K content was observed. The torrefaction temperature was too severe at long durations, as seen by EY's sharp drop after 30 and 60 min. The ANN-developed model was excellent in predicting the SY, EY, and EF based on the provided input (K content and torrefaction duration). These results provide a starting point for integrating machine learning in bioenergy. Given the upgraded wood properties achieved through this method, the torrefied wood can subsequently be valorized in different applications, whether as a fossil fuel replacement or for co-firing and co-gasification. Torrefaction of wood boards prior to grinding substantially reduces the costs and energy consumption of the process. Therefore, the tested method shows great potential for industrial application. Further studies should evaluate the behavior of different wood species with increasing K content.

CRediT authorship contribution statement

Larissa Richa: Visualization, Validation, Methodology, Investigation, Formal analysis, Data curation. Baptiste Colin: Writing – review & editing, Validation, Investigation. Anélie Pétrissans: Writing – review & editing, Supervision, Resources, Project administration, Investigation, Funding acquisition, Formal analysis, Conceptualization. Ciera Wallace: Investigation, Data curation. Jasmine Wolfgram: Formal analysis, Data curation. Rafael L. Quirino: Project administration, Formal analysis, Data curation. Wei-Hsin Chen: Writing – review & editing, Software, Investigation, Funding acquisition, Formal analysis. Mathieu Pétrissans: Writing – review & editing, Supervision, Resources, Project administration, Investigation, Funding acquisition.

Declaration of Competing Interest

The authors declare that they have no known competing financial interests or personal relationships that could have appeared to influence the work reported in this paper.

Data availability

Data will be made available on request.

Acknowledgments

The authors gratefully acknowledge the financial support under the program ANR-11-LABEX-0002-01 (Lab of Excellence ARBRE) in France, the National Science Foundation (NSF) under the grant NSF-IRES 1952402 (I-CEMITURE (International-CEMITURE)) awarded by the NSF Office of International Science & Engineering (OISE), Georgia Southern University USA; Thomas Jefferson Fund of the Embassy of France in the United States and the FACE Foundation. The authors also acknowledge the financial support of the National Science and Technology Council, Taiwan, R.O.C., under contracts NSTC 112-2218-E-006-025- and NSTC 112-2218-E-002-052-, for this research.

References

- Kreps BH. The rising costs of fossil-fuel extraction: an energy crisis that will not go away. Am J Econ Sociol May 2020;79(3):695–717. https://doi.org/10.1111/ pigs 13236
- [2] Sebestyén V. Renewable and sustainable energy reviews: environmental impact networks of renewable energy power plants. Renew Sustain Energy Rev Nov. 2021; 151:111626, https://doi.org/10.1016/j.rser.2021.111626.
- [3] Danish, Wang Z. Does biomass energy consumption help to control environmental pollution? Evidence from BRICS countries. Sci Total Environ Jun. 2019;670: 1075–83. https://doi.org/10.1016/j.scitotenv.2019.03.268.
- 1075–83. https://doi.org/10.1016/j.scitotenv.2019.03.268.
 Yu S, Wang L, Li Q, Zhang Y, Zhou H. Sustainable carbon materials from the pyrolysis of lignocellulosic biomass. Mater Today Sustain Nov. 2022;19:100209. https://doi.org/10.1016/j.mtsust.2022.100209.

- [5] Yu S, Yang X, Li Q, Zhang Y, Zhou H. Breaking the temperature limit of hydrothermal carbonization of lignocellulosic biomass by decoupling temperature and pressure. Green Energy Environ Aug. 2023;8(4):1216–27. https://doi.org/ 10.1016/j.gee.2023.01.001.
- [6] Yu S, Dong X, Zhao P, Luo Z, Sun Z, Yang X, et al. Decoupled temperature and pressure hydrothermal synthesis of carbon sub-micron spheres from cellulose. Nat Commun Jun. 2022;13(1):3616. https://doi.org/10.1038/s41467-022-31352-x.
- [7] Chen W-H, Lin B-J, Lin Y-Y, Chu Y-S, Ubando AT, Show PL, et al. Progress in biomass torrefaction: principles, applications and challenges. Prog Energy Combust Sci Jan. 2021;82:100887. https://doi.org/10.1016/j.pecs.2020.100887.
- [8] Niu Y, Lv Y, Lei Y, Liu S, Liang Y, Wang D, et al. Biomass torrefaction: properties, applications, challenges, and economy. Renew Sustain Energy Rev Nov. 2019;115: 109395. https://doi.org/10.1016/j.rser.2019.109395.
- [9] Chen C, Yang R, Wang X, Qu B, Zhang M, Ji G, et al. Effect of in-situ torrefaction and densification on the properties of pellets from rice husk and rice straw. Chemosphere Feb. 2022;289:133009. https://doi.org/10.1016/j. chemosphere 2021.133009.
- [10] Wang L, Riva L, Skreiberg Ø, Khalil R, Bartocci P, Yang Q, et al. Effect of Torrefaction on properties of pellets produced from woody biomass. Energy Fuel Dec. 2020;34(12):15343–54. https://doi.org/10.1021/acs.energyfuels.0c02671.
- [11] Arias B, Pevida C, Fermoso J, Plaza MG, Rubiera F, Pis JJ. Influence of torrefaction on the grindability and reactivity of woody biomass. Fuel Process Technol Feb. 2008;89(2):169–75. https://doi.org/10.1016/j.fuproc.2007.09.002.
- [12] Manouchehrinejad M, Van Giesen I, Mani S. Grindability of torrefied wood chips and wood pellets. Fuel Process Technol Dec. 2018;182:45–55. https://doi.org/ 10.1016/j.fuproc.2018.10.015.
- [13] Batidzirai B, Van Der Hilst F, Meerman H, Junginger MH, Faaij APC. Optimization potential of biomass supply chains with torrefaction technology. Biofuels Bioprod Biorefin Mar. 2014;8(2):253–82. https://doi.org/10.1002/bbb.1458.
- [14] Chen C, Qu B, Wang W, Wang W, Ji G, Li A. Rice husk and rice straw torrefaction: properties and pyrolysis kinetics of raw and torrefied biomass. Environ Technol Innov Nov. 2021;24:101872. https://doi.org/10.1016/ji.eti.2021.101872.
- [15] Yun H, Clift R, Bi X. Environmental and economic assessment of torrefied wood pellets from British Columbia. Energ Conver Manage Mar. 2020;208:112513. https://doi.org/10.1016/j.enconman.2020.112513.
- [16] Olugbade TO, Ojo OT. Biomass Torrefaction for the production of high-grade solid biofuels: a review. Bioenergy Res Dec. 2020;13(4):999–1015. https://doi.org/ 10.1007/s12155-020-10138-3.
- [17] Li J, Brzdekiewicz A, Yang W, Blasiak W. Co-firing based on biomass torrefaction in a pulverized coal boiler with aim of 100% fuel switching. Appl Energy Nov. 2012; 99:344–54. https://doi.org/10.1016/j.apenergy.2012.05.046.
- [18] Johnson R, Vishwakarma K, Hossen MdS, Kumar V, Shackira AM, Puthur JT, et al. Potassium in plants: growth regulation, signaling, and environmental stress tolerance. Plant Physiol Biochem Feb. 2022;172:56–69. https://doi.org/10.1016/j. plaphy.2022.01.001.
- [19] Clery DS, Mason PE, Rayner CM, Jones JM. The effects of an additive on the release of potassium in biomass combustion. Fuel Feb. 2018;214:647–55. https://doi.org/ 10.1016/j.fuel.2017.11.040.
- [20] Liu X, Yi C, Chen L, Niu R, Mi T, Wu Q, et al. Synergy of steam reforming and K2CO3 modification on wood biomass pyrolysis. Cellulose Jul. 2019;26(10): 6049–60. https://doi.org/10.1007/s10570-019-02480-3.
- [21] Xu ZY, Wang RZ, Yang C. Perspectives for low-temperature waste heat recovery. Energy Jun. 2019;176:1037–43. https://doi.org/10.1016/j.energy.2019.04.001.
- [22] Wang Z, Wang F, Cao J, Wang J. Pyrolysis of pine wood in a slowly heating fixed-bed reactor: potassium carbonate versus calcium hydroxide as a catalyst. Fuel Process Technol Aug. 2010;91(8):942–50. https://doi.org/10.1016/j.fixeres 2000.00.01.
- [23] Hwang H, Oh S, Cho T-S, Choi I-G, Choi JW. Fast pyrolysis of potassium impregnated poplar wood and characterization of its influence on the formation as well as properties of pyrolytic products. Bioresour Technol Dec. 2013;150:359–66. https://doi.org/10.1016/j.biortech.2013.09.132.
- [24] Guo F, Liu Y, Wang Y, Li X, Li T, Guo C. Pyrolysis kinetics and behavior of potassium-impregnated pine wood in TGA and a fixed-bed reactor. Energ Conver Manage Dec. 2016;130:184–91. https://doi.org/10.1016/j. encomman 2016;10.055
- [25] Carvalho A, Rabaçal M, Costa M, Alzueta MU, Abián M. Effects of potassium and calcium on the early stages of combustion of single biomass particles. Fuel Dec. 2017;209:787–94. https://doi.org/10.1016/j.fuel.2017.08.045.
- [26] Hu Q, Yang H, Wu Z, Lim CJ, Bi XT, Chen H. Experimental and modeling study of potassium catalyzed gasification of woody char pellet with CO2. Energy Mar. 2019; 171:678–88. https://doi.org/10.1016/j.energy.2019.01.050.
- [27] Chia CH, Singh BP, Joseph S, Graber ER, Munroe P. Characterization of an enriched biochar. J Anal Appl Pyrolysis Jul. 2014;108:26–34. https://doi.org/10.1016/j. jaap.2014.05.021.
- [28] Jaiswal DK, Verma JP, Prakash S, Meena VS, Meena RS. Potassium as an important plant nutrient in sustainable agriculture: A state of the art. In: Meena VS, Maurya BR, Verma JP, Meena RS, editors. Potassium solubilizing microorganisms for sustainable agriculture. New Delhi: Springer India; 2016. p. 21–9. https://doi. org/10.1007/978-81-322-2776-2 2.
- [29] Tsai WT, Chang CY, Wang SY, Chang CF, Chien SF, Sun HF. Preparation of activated carbons from corn cob catalyzed by potassium salts and subsequent gasification with CO2. Bioresour Technol Jun. 2001;78(2):203–8. https://doi.org/ 10.1016/S0960-8524(00)00111-5.
- [30] Khazraie Shoulaifar T, DeMartini N, Karlström O, Hupa M. Impact of organically bonded potassium on torrefaction: part 1. Experimental. Fuel Feb. 2016;165: 544–52. https://doi.org/10.1016/j.fuel.2015.06.024.

[31] Silveira EA, Macedo LA, Rousset P, Candelier K, Galvão LGO, Chaves BS, et al. A potassium responsive numerical path to model catalytic torrefaction kinetics. Energy Jan. 2022;239:122208. https://doi.org/10.1016/j.energy.2021.122208.

- [32] Nishimura M, Iwasaki S, Horio M. The role of potassium carbonate on cellulose pyrolysis. J Taiwan Inst Chem Eng Nov. 2009;40(6):630–7. https://doi.org/ 10.1016/j.jtice.2009.05.005.
- [33] Simonic M, Goricanec D, Urbancl D. Impact of torrefaction on biomass properties depending on temperature and operation time. Sci Total Environ Oct. 2020;740: 140086. https://doi.org/10.1016/j.scitotenv.2020.140086.
- [34] Wannapeera J, Fungtammasan B, Worasuwannarak N. Effects of temperature and holding time during torrefaction on the pyrolysis behaviors of woody biomass. J Anal Appl Pyrolysis Sep. 2011;92(1):99–105. https://doi.org/10.1016/j. iaan 2011.04.010
- [35] Prade T, Svensson S-E, Andersson A, Mattsson JE. Biomass and energy yield of industrial hemp grown for biogas and solid fuel. Biomass Bioenergy Jul. 2011;35 (7):3040–9. https://doi.org/10.1016/j.biombioe.2011.04.006.
- [36] Singh S, Chakraborty JP, Mondal MK. Optimization of process parameters for torrefaction of Acacia nilotica using response surface methodology and characteristics of torrefied biomass as upgraded fuel. Energy Nov. 2019;186: 115865. https://doi.org/10.1016/j.energy.2019.115865.
- [37] Huo Y, Bouffard F, Joós G. Decision tree-based optimization for flexibility management for sustainable energy microgrids. Appl Energy May 2021;290: 116772. https://doi.org/10.1016/j.apenergy.2021.116772.
- [38] Aniza R, Chen W-H, Yang F-C, Pugazhendh A, Singh Y. Integrating Taguchi method and artificial neural network for predicting and maximizing biofuel production via torrefaction and pyrolysis. Bioresour Technol Jan. 2022;343:126140. https://doi. org/10.1016/j.biortech.2021.126140.
- [39] Manatura K, Chalermsinsuwan B, Kaewtrakulchai N, Kwon EE, Chen W-H. Machine learning and statistical analysis for biomass torrefaction: a review. Bioresour Technol Feb. 2023;369:128504. https://doi.org/10.1016/j.biortech.2022.128504.
- [40] Xing S, Yuan H, Huhetaoli Y, Qi P, Lv Z Yuan, Chen Y. Characterization of the decomposition behaviors of catalytic pyrolysis of wood using copper and potassium over thermogravimetric and Py-GC/MS analysis. Energy Nov. 2016;114:634–46. https://doi.org/10.1016/j.energy.2016.07.154.
- [41] Zhao L, Zhou H, Xie Z, Li J, Yin Y. Effects of potassium on solid products of peanut shell torrefaction. Energy Sour Part A: Rec Utiliz Environ Effects May 2020;42(10): 1235–46. https://doi.org/10.1080/15567036.2019.1602232.
- [42] de Macedo LA, Commandré J-M, Rousset P, Valette J, Pétrissans M. Influence of potassium carbonate addition on the condensable species released during wood torrefaction. Fuel Process Technol Jan. 2018;169:248–57. https://doi.org/ 10.1016/j.fjuproc.2017.10.012.
- [43] Basu P, Sadhukhan AK, Gupta P, Rao S, Dhungana A, Acharya B. An experimental and theoretical investigation on torrefaction of a large wet wood particle. Bioresour Technol May 2014;159:215–22. https://doi.org/10.1016/j. biortech.2014.02.105.
- [44] Perré P, Rémond R, Turner I. A comprehensive dual-scale wood torrefaction model: application to the analysis of thermal run-away in industrial heat treatment processes. Int J Heat Mass Transf Sep. 2013;64:838–49. https://doi.org/10.1016/j. iiheatmasstransfer.2013.03.066.
- [45] Ackerman Drs Joe, Cicek N. Recovering agricultural nutrients (potassium and phosphorus) from biomass ash: a review of literature. 2017. https://doi.org/ 10.13140/BG.2.2.24745.85605.
- [46] Tokuşoglu O, Uunal MK. Biomass nutrient profiles of three microalgae: Spirulina platensis, Chlorella vulgaris, and Isochrisis galbana. J Food Sci May 2003;68(4): 1144–8. https://doi.org/10.1111/j.1365-2621.2003.tb09615.x.
- [47] Duxbury M. Determination of minerals in apples by ICP-AES. J Chem Educ Oct. 2003;80(10):1180. https://doi.org/10.1021/ed080p1180.
 [48] Musa Özcan M. Determination of the mineral compositions of some selected oil-
- [48] Musa Ozcan M. Determination of the mineral compositions of some selected oil-bearing seeds and kernels using inductively coupled plasma atomic emission spectrometry (ICP-AES). Grasas Aceites Jun. 2006;57(2):211–8. https://doi.org/10.3989/gya.2006.v57.i2.39.
- [49] Tondi G, Thevenon MF, Mies B, Standfest G, Petutschnigg A, Wieland S. Impregnation of scots pine and beech with tannin solutions: effect of viscosity and wood anatomy in wood infiltration. Wood Sci Technol May 2013;47(3):615–26. https://doi.org/10.1007/s00226-012-0524-5.
- [50] Chen W-H, Aniza R, Arpia AA, Lo H-J, Hoang AT, Goodarzi V, et al. A comparative analysis of biomass torrefaction severity index prediction from machine learning. Appl Energy Oct. 2022;324:119689. https://doi.org/10.1016/j. apenergy.2022.119689.
- [51] Yi L, Feng J, Qin Y-H, Li W-Y. Prediction of elemental composition of coal using proximate analysis. Fuel Apr. 2017;193:315–21. https://doi.org/10.1016/j. fuel.2016.12.044.
- [52] NF EN ISO 18122. Solid biofuels Determination of ash content. Dec. 2015.
- [53] NF EN ISO 18123. Solid biofuels Determination of the content of volatile matter. Dec. 2015.
- [54] Granados DA, Basu P, Chejne F, Nhuchhen DR. Detailed investigation into Torrefaction of wood in a two-stage inclined rotary Torrefier. Energy Fuel Jan. 2017;31(1):647–58. https://doi.org/10.1021/acs.energyfuels.6b02524.
- [55] Boutaieb M, Guiza M, Román S, Ledesma Cano B, Nogales S, Ouederni A. Hydrothermal carbonization as a preliminary step to pine cone pyrolysis for bioenergy production. C R Chim Feb. 2021;23(11–12):607–21. https://doi.org/ 10.5802/crchim.47.
- [56] Telmo C, Lousada J. Heating values of wood pellets from different species. Biomass Bioenergy Jul. 2011;35(7):2634–9. https://doi.org/10.1016/j. biombioe.2011.02.043.

- [57] NF EN ISO 18125. Solid biofuels Determination of calorific value. Jul. 2017 [Online]. Available: https://viewerbdc.afnor.org/html/display/FXrT1lEaYyQ1.
- [58] Chen W-H, Huang M-Y, Chang J-S, Chen C-Y, Lee W-J. An energy analysis of torrefaction for upgrading microalga residue as a solid fuel. Bioresour Technol Jun. 2015;185:285–93. https://doi.org/10.1016/j.biortech.2015.02.095.
- [59] Chen W-H, Hsu H-J, Kumar G, Budzianowski WM, Ong HC. Predictions of biochar production and torrefaction performance from sugarcane bagasse using interpolation and regression analysis. Bioresour Technol Dec. 2017;246:12–9. https://doi.org/10.1016/j.biortech.2017.07.184.
- [60] Chen W-H, Lo H-J, Aniza R, Lin B-J, Park Y-K, Kwon EE, et al. Forecast of glucose production from biomass wet torrefaction using statistical approach along with multivariate adaptive regression splines, neural network and decision tree. Appl Energy Oct. 2022;324:119775. https://doi.org/10.1016/j.apenergy.2022.119775.
- [61] Andersson M, Pahlsson A-MB, Berlin G, Falkengren-Grerup U, Tyler G. Environment and mineral nutrients of beech (Fagus sylvatica L.) in South Sweden. Flora 1989;183(5–6):405–15. https://doi.org/10.1016/S0367-2530(17)31572-4.
- [62] Albert R, Pescoller-Tiefenthaler G. Nutrient content and ionic pattern in beech (Fagus sylvatica L.) from natural stands in eastern Austria and ecological implications. Vegetatio Jul. 1992;101(1):81–95. https://doi.org/10.1007/ BED0031017
- [63] Saleh SB, Hansen BB, Jensen PA, Dam-Johansen K. Influence of biomass chemical properties on torrefaction characteristics. Energy Fuel Dec. 2013;27(12):7541–8. https://doi.org/10.1021/ef401788m.
- [64] Fernandes J, Kjellow AW, Henriksen O. Modeling and optimization of the supercritical wood impregnation process—focus on pressure and temperature. J Supercritic Fluids Jun. 2012;66:307–14. https://doi.org/10.1016/j. supflu.2012.03.003.
- [65] Richa L, Colin B, Pétrissans A, Wallace C, Hulette A, Quirino RL, et al. Catalytic and char-promoting effects of potassium on lignocellulosic biomass torrefaction and pyrolysis. Environ Technol Innov May 2023:103193. https://doi.org/10.1016/j. eti.2023.103193.
- [66] Määttänen M, Tikka DP. Determination of phenomena involved in impregnation of softwood chips. Part 2: alkali uptake, alkali consumption and impregnation yield. Nordic Pulp & Paper Res J Aug. 2012;27(3):559–67. https://doi.org/10.3183/ nppri-2012-27-03-p559-567.
- [67] Ohliger A, Förster M, Kneer R. Torrefaction of beechwood: a parametric study including heat of reaction and grindability. Fuel Feb. 2013;104:607–13. https:// doi.org/10.1016/j.fuel.2012.06.112.
- [68] Safar M, Lin B-J, Chen W-H, Langauer D, Chang J-S, Raclavska H, et al. Catalytic effects of potassium on biomass pyrolysis, combustion and torrefaction. Appl Energy Feb. 2019;235:346–55. https://doi.org/10.1016/j.apenergy.2018.10.065.
- [69] Quirino RL, Richa L, Petrissans A, Teixeira PR, Durrell G, Hulette A, et al. Comparative study of atmosphere effect on wood torrefaction. Fibers Mar. 2023;11 (3):27. https://doi.org/10.3390/fib11030027.
- [70] Cardona S, Gallego LJ, Valencia V, Martínez E, Rios LA. Torrefaction of eucalyptustree residues: a new method for energy and mass balances of the process with the best torrefaction conditions. Sustain Energy Technol Assess Feb. 2019;31:17–24. https://doi.org/10.1016/j.jseta.2018.11.002
- [71] Chen W-H, Huang M-Y, Chang J-S, Chen C-Y. Thermal decomposition dynamics and severity of microalgae residues in torrefaction. Bioresour Technol Oct. 2014; 169:258–64. https://doi.org/10.1016/j.biortech.2014.06.086.
- [72] Chen W-H, Huang M-Y, Chang J-S, Chen C-Y. Torrefaction operation and optimization of microalga residue for energy densification and utilization. Appl Energy Sep. 2015;154:622–30. https://doi.org/10.1016/j.apenergy.2015.05.068.
- [73] Chen W-H, Cheng C-L, Show P-L, Ong HC. Torrefaction performance prediction approached by torrefaction severity factor. Fuel Sep. 2019;251:126–35. https://doi.org/10.1016/j.fuel.2019.04.047.
- [74] Miao M, Deng B, Kong H, Yang H, Lyu J, Jiang X, et al. Effects of volatile matter and oxygen concentration on combustion characteristics of coal in an oxygenenriched fluidized bed. Energy Apr. 2021;220:119778. https://doi.org/10.1016/j. energy.2021.119778.
- [75] Cahyanti MN, Doddapaneni TRKC, Kikas T. Biomass torrefaction: an overview on process parameters, economic and environmental aspects and recent advancements. Bioresour Technol Apr. 2020;301:122737. https://doi.org/ 10.1016/j.biortech.2020.122737.
- [76] Sharifi M, Cheema M, McVicar K, LeBlanc L, Fillmore S. Evaluation of liming properties and potassium bioavailability of three Atlantic Canada wood ash

- sources. Can J Plant Sci Nov. 2013;93(6):1209–16. https://doi.org/10.4141/cips2013-168.
- [77] Cheng Y, Jiang H, Zhang X, Cui J, Song C, Li X. Effects of coal rank on physicochemical properties of coal and on methane adsorption. Int J Coal Sci Technol Jun. 2017;4(2):129–46. https://doi.org/10.1007/s40789-017-0161-6.
- [78] Iacovidou E, Hahladakis J, Deans I, Velis C, Purnell P. Technical properties of biomass and solid recovered fuel (SRF) co-fired with coal: impact on multidimensional resource recovery value. Waste Manag Mar. 2018;73:535–45. https:// doi.org/10.1016/j.wasman.2017.07.001.
- [79] Schmidt Hans-Peter. European Biochar Certificate (EBC) guidelines version 6.1. 2015. https://doi.org/10.13140/RG.2.1.4658.7043.
- [80] Richards AP, Haycock D, Frandsen J, Fletcher TH. A review of coal heating value correlations with application to coal char, tar, and other fuels. Fuel Jan. 2021;283: 118942. https://doi.org/10.1016/j.fuel.2020.118942.
- [81] Prins MJ, Ptasinski KJ, Janssen FJJG. More efficient biomass gasification via torrefaction. Energy Dec. 2006;31(15):3458–70. https://doi.org/10.1016/j. energy 2006.03.008
- [82] Prins M, Ptasinski K, Janssen F. From coal to biomass gasification: comparison of thermodynamic efficiency. Energy Jul. 2007;32(7):1248–59. https://doi.org/ 10.1016/j.energy.2006.07.017
- [83] Gan YY, Ong HC, Ling TC, Chen W-H, Chong CT. Torrefaction of de-oiled Jatropha seed kernel biomass for solid fuel production. Energy Mar. 2019;170:367–74. https://doi.org/10.1016/j.energy.2018.12.026.
- [84] Yu S, Park J, Kim M, Kim H, Ryu C, Lee Y, et al. Improving energy density and grindability of wood pellets by dry torrefaction. Energy Fuel Sep. 2019;33(9): 8632–9. https://doi.org/10.1021/acs.energyfuels.9b01086.
- [85] Ben H, Ragauskas AJ. Torrefaction of loblolly pine. Green Chem 2012;14(1):72–6. https://doi.org/10.1039/C1GC15570A.
- [86] Umar DF, Usui H, Daulay B. Change of combustion characteristics of Indonesian low rank coal due to upgraded brown coal process. Fuel Process Technol Nov. 2006;87(11):1007–11. https://doi.org/10.1016/j.fuproc.2006.07.010.
- [87] Begum N, Chakravarty D, Das BS. Estimation of gross calorific value of bituminous coal using various coal properties and reflectance spectra. Int J Coal Preparat Utiliz Apr. 2022;42(4):979–85. https://doi.org/10.1080/19392699.2019.1621301.
- [88] Grammelis P, Margaritis N, Karampinis E. Solid fuel types for energy generation. In: Fuel flexible energy generation. Elsevier; 2016. p. 29–58. https://doi.org/ 10.1016/B978-1-78242-378-2.00002-X.
- [89] Tumuluru Jaya Shankar, Wright Christopher T, Boardman Richard D, Yancey Neal A, Sokhansanj Shahab. A review on biomass classification and composition, cofiring issues and pretreatment methods. In: 2011 Louisville, Kentucky, August 7 -August 10, 2011, American Society of Agricultural and Biological Engineers; 2011. https://doi.org/10.13031/2013.37191.
- 90] García Nieto PJ, García-Gonzalo E, Sánchez Lasheras F, Paredes-Sánchez JP, Riesgo Fernández P. Forecast of the higher heating value in biomass torrefaction by means of machine learning techniques. J Comp Appl Math Sep. 2019;357:284–301. https://doi.org/10.1016/j.cam.2019.03.009.
- [91] Abdulyekeen KA, Daud WMAW, Patah MFA, Abnisa F. Torrefaction of organic municipal solid waste to high calorific value solid fuel using batch reactor with helical screw induced rotation. Bioresour Technol Nov. 2022;363:127974. https://doi.org/10.1016/j.biortech.2022.127974
- [92] Kambo HS, Dutta A. A comparative review of biochar and hydrochar in terms of production, physico-chemical properties and applications. Renew Sustain Energy Rev May 2015;45:359–78. https://doi.org/10.1016/j.rser.2015.01.050.
 [94] Yang H, Yan R, Chen H, Lee DH, Zheng C. Characteristics of hemicellulose,
- [94] Yang H, Yan R, Chen H, Lee DH, Zheng C. Characteristics of hemicellulose, cellulose and lignin pyrolysis. Fuel Aug. 2007;86(12–13):1781–8. https://doi.org/ 10.1016/j.fuel.2006.12.013
- [95] Peng J, Wang J, Bi XT, Lim CJ, Sokhansanj S, Peng H, et al. Effects of thermal treatment on energy density and hardness of torrefied wood pellets. Fuel Process Technol Jan. 2015;129:168–73. https://doi.org/10.1016/j.fuproc.2014.09.010.
- [97] Onsree T, Tippayawong N. Machine learning application to predict yields of solid products from biomass torrefaction. Renew Energy Apr. 2021;167:425–32. https://doi.org/10.1016/j.renene.2020.11.099.
- [98] Chiou B-S, Valenzuela-Medina D, Bilbao-Sainz C, Klamczynski AP, Avena-Bustillos RJ, Milczarek RR, et al. Torrefaction of almond shells: effects of torrefaction conditions on properties of solid and condensate products. Ind Crop Prod Aug. 2016;86:40–8. https://doi.org/10.1016/j.indcrop.2016.03.030.